

Journal Pre-proof

Tectonic framework of surface and blind structures from neotectonic and geophysical (gravimetry) analyses, Central Andes of Argentina

J. Alcacer, M. Rothis, F. Haro, B. Colavitto, H.N. Vargas, M. Vargas, M. Onorato, P. Blanc, S. Miranda, L. Perucca



PII: S0895-9811(23)00183-9

DOI: <https://doi.org/10.1016/j.jsames.2023.104372>

Reference: SAMES 104372

To appear in: *Journal of South American Earth Sciences*

Received Date: 29 November 2022

Revised Date: 18 April 2023

Accepted Date: 24 April 2023

Please cite this article as: Alcacer, J., Rothis, M., Haro, F., Colavitto, B., Vargas, H.N., Vargas, M., Onorato, M., Blanc, P., Miranda, S., Perucca, L., Tectonic framework of surface and blind structures from neotectonic and geophysical (gravimetry) analyses, Central Andes of Argentina, *Journal of South American Earth Sciences* (2023), doi: <https://doi.org/10.1016/j.jsames.2023.104372>.

This is a PDF file of an article that has undergone enhancements after acceptance, such as the addition of a cover page and metadata, and formatting for readability, but it is not yet the definitive version of record. This version will undergo additional copyediting, typesetting and review before it is published in its final form, but we are providing this version to give early visibility of the article. Please note that, during the production process, errors may be discovered which could affect the content, and all legal disclaimers that apply to the journal pertain.

© 2023 Published by Elsevier Ltd.

TECTONIC FRAMEWORK OF SURFACE AND BLIND STRUCTURES FROM NEOTECTONIC AND GEOPHYSICAL (GRAVIMETRY) ANALYSES, CENTRAL ANDES OF ARGENTINA

Alcacer, J.^{1,2}, Rothis, M.^{1,2}, Haro, F.^{1,2}, Colavitto, B.^{1,3}, Vargas, H.N.¹, Vargas, M.^{1,2},
Onorato, M.^{1,2}, Blanc, P.¹, Miranda, S.⁴, Perucca, L.^{1,2*}

¹*Gabinete de Neotectónica y Geomorfología. Instituto de Geología Emiliano P. Aparicio (INGEO-Facultad de Ciencias Exactas, Físicas y Naturales, Universidad Nacional de San Juan), Av. Ignacio de La Roza y Meglioli, 5400 San Juan, Argentina. E-mail: lauraperucca@unsj-cuim.edu.ar*

²*Consejo Nacional de Investigaciones Científicas y Técnicas (CONICET)*

⁴*Departamento Geofísica y Astronomía (Facultad de Ciencias Exactas, Físicas y Naturales, Universidad Nacional de San Juan) Av. Ignacio de La Roza y Meglioli 5400-San Juan.*

**Corresponding author*

Abstract

This work describes new evidence of N-S and oblique trending surface and blind structures in the La Cantera-Gualilán tectonic depression in the Central Precordillera, San Juan Province, Argentina. Two main N-S Quaternary thrusts cross longitudinally the valley located ~60 km west of San Juan city (30° 50' - 31° 17' S and 68° 55' - 69° 05' W). One of them is located in the eastern piedmont of the Sierra de La Invernada (San Juan Fault) and the other in the western piedmont of the Sierra de La Cantera (La Cantera Fault System), although the northward continuation of this structure has not yet been confirmed.

Besides, a smooth water divide or "portezuelo" controlled by an oblique transpressive structure (Divisadero Coba Rubia Fault) separates two N-S elongated river basins with opposite water flow directions. One of these is the Gualilán River, which flows from south to north, and the other corresponds to the La Cantera River, running from north to south.

In the present work, we describe some new natural exposures and subtle geomorphological evidence of Quaternary structures identified in the Gualilán-La Cantera tectonic depression.

We also use regional and local gravity data to analyze and interpret gravity anomalies related to these surface or blind active structures. Then, based on our geologic and geophysical interpretations, we infer the presence of several, buried cross-strike structures with NW and NE trends, one of them coincident with the drainage divide between the Gualilán and La Cantera opposite river basins, possibly related to the Coba Rubia Fault. Also, we suggest the northward continuation of the La Cantera Fault System (LCFS) as a buried structure in coincidence with the Gualilán River alluvial plain. In this sense, the gravity response of the basement and these river sub-basins shows a close relationship with the surface and subsurface structures. We propose that the oblique structures could represent pre-existing crustal fabrics reactivated during the Andean orogeny, segmenting the N-S Precordillera fold and thrust belt system. Finally, according to the analyzed neotectonic and gravimetric features, we consider the La Cantera-Gualilán Valley as a potentially seismogenic source in this intraplate portion of the Andean Precordillera, crossed by several N-S and oblique surficial and buried/blind active structures. These tectonic features could play a significant role in a regional seismic hazard assessment.

Keywords: Neotectonics , Gravimetry, Precordillera, Andean Ranges, Oblique structures

1. Introduction

Characterization of surface and buried/blind active faults requires multidisciplinary approaches. These include, among others, satellite mapping, fieldwork, sampling for dating, and sedimentological analyses. Structures with low activity rates or long interseismic intervals can be hidden at the surface by erosion or sedimentation. Detailed mapping of active faults not expressed at the surface can also be problematic for any seismic hazard assessment. In this way, geophysical surveys such as gravimetry can assist and provide information on the location of active structures in the subsurface.

The Andean Precordillera of western Argentina is a first-order morphotectonic unit of the Chilean-Pampean flat slab between 27° S and 34° S and is one of the most seismically active zones of thrust tectonics in the world. Most of the physiographic features of Precordillera are strongly controlled by the Mio-Pliocene structures resulting from the Andean orogeny. These are large and actively growing mountain ranges trending N-S flanked by thrusts (Allmendinger et al., 1990; Cristallini and Ramos, 2000, among others).

The study area is located in a tectonic valley between the Sierra de La Crucecita-La Cantera to the east and the Sierra de La Invernada to the west (30° 50'- 31° 17' S and 68° 50'- 69° 05' W), in the Central Precordillera of San Juan, Argentina (Figure 1a). The Sierra de La Crucecita-La Cantera is a ~N-S mountain range with maximum elevations of 2000 m asl and 3139 m asl, respectively. The Sierra de La Invernada has a NNE trend and a maximum altitude of 3705 m asl. This tectonic valley extends from the Puesto Pachaco locality in the right margin of the San Juan River (1190 m asl) in the south, to the Pampa de Gualilán (1620 m asl) in the north (Figure 1a, b). The depression is also segmented into two N-S river basins with opposite flow directions: The Gualilán River basin, whose main river runs from south

to north, and the La Cantera River basin, which runs from north to south. These river basins are considered by Suriano et al. (2015) as collector-conoid river systems. This term is used to identify deposits resulting from small rivers that drain the intermountain valleys longitudinally forming prominent conoids when reaching the transfer systems that cross Precordillera (in this case, the San Juan River to the south) or closed basins (endorheic) as the Pampa de Gualilán (to the north). These collector-conoid systems are strongly controlled by the active structures that cross and limit these depressions, mainly affecting the eastern piedmont of Sierra de La Invernada and the western piedmont of the Sierra de La Cantera (Whitney and Bastías 1984). Quaternary deformations identified in both piedmonts modify drainage patterns, as has been described by Millán and Perucca (2011) and Perucca et al. (2014a, b; 2015).

Vargas et al. (2020) made a morphometric and morphotectonic characterization of the Gualilán-La Cantera river basins, complemented by an ongoing stream piracy process analysis. These authors suggested that the La Cantera River may capture the headwaters of the Gualilán River shortly. Also, they mentioned a possible structure trending ~E–W coincident with the headwaters of both N–S rivers, which would influence their dynamics. Oblique structures segmenting this portion of Central Precordillera were also suggested by Japas (1998), Ré et al. (2001), Japas et al. (2002), and Ré and Japas (2004) and then confirmed as reactivated pre-Neogene sinistral cross-strike structures in the Gualilán area by Oriolo et al. (2013, 2015).

In this work, a neotectonic analysis of the Gualilán-La Cantera tectonic depression is carried out. Several subtle morphotectonic features in the Gualilán river plain suggest the northward continuation of the La Cantera Fault System as a blind structure. In addition, two W-E north-verging Quaternary reverse faults observed in a natural exposure at the water divide

(Portezuelo Divisadero Coba Rubia) of both river basins are described as complementing the main N-S Quaternary structures already known (Figure 1).

Swath profiles constitutes simple tools that helped to recognize and to identify surface scarps, slope variations, river incisions and other topographic effects in a concise way. In other words, to expeditiously evaluate the effects of vertical movements on the topography of the valley, slope of rivers, watersheds, etc.

In addition, this research tries to define, through the processing and analysis of regional and local gravity data, the northward continuation of the La Cantera Fault System as a blind structure and the oblique geological structures segmenting this area of Precordillera. Gravity data extracted from global geopotential models provide an invaluable tool for regional-scale tectonic-geophysical analysis achieving homogeneous data coverage in those areas where ground gravity data maintain a skewed and dispersed distribution. The Residual Bouguer anomalies analysis based on different filtering techniques in the space domain (Bandpass and Butterworth) allows for defining the spatial continuity of blind structures (Pacino, 2007; Rojas Vera et al., 2010; Rivas et al., 2021).

The geophysical and geological analyses would confirm the existence of blind structures limiting and controlling tectonic depressions and basement highs. Then, the gravity signature associated with structural features defines the spatial continuity of these neotectonic features in those sectors where field evidence is unclear or blind structures are present.

Finally, this work aims to improve the knowledge about the active structures (surface and/or blind) in an intermountain depression located scarcely 70 km northwest of San Juan city (> 800,000 inhabitants) and close to four hydroelectric dams in the region.

2. Geological setting

2.1 Tectonic setting

In the current geotectonic setting of convergence between the Nazca and South American plates (southern portion segment of the Central Andes), the Pampean flat-slab subduction began at this latitude (27°-34°S), between 18 and 12 Ma (Jordan et al., 1983; Yáñez et al., 2001; Ramos et al., 2002). Intense seismic activity and the absence of active volcanoes characterize the region (Cahill and Isacks, 1992), related to active faults that thrust the Paleozoic to Neogene sequences over Quaternary alluvial deposits. In this way, much evidence of Quaternary deformation has been described at these latitudes (Perucca et al., 1999; Costa et al., 2000; Perucca et al., 2012, 2014a, b, 2015; Perucca and Vargas, 2014, Audemard et al., 2016, Tejada et al., 2021, among others).

The Precordillera is a Paleozoic orogenic unit subdivided according to its structural style in Western, Central, and Eastern Precordillera (Ortiz and Zambrano, 1981) (Figure 1a). The study area is in the Central Precordillera, which constitutes a N-S trending, E-verging thin-skinned fold and thrust belt, and imbricated structures rooted at 10–15 km deep main *décollement* (Zapata and Allmendinger, 1996; Ramos, 1988). Cenozoic rocks are preserved in the footwalls of major thrusts (Jordan et al., 1993; Alonso et al., 2005), being differentially eroded to form N-S trending intermountain valleys between the thrust-generated ranges (Levina et al., 2014) (Figure 1c).

Levina et al. (2014) evaluated the Cenozoic basin fill of the frontal sector of the Precordillera foreland basin in three valleys located along the San Juan River (one of them, the La Cantera Valley), concluding that the Neogene successions located in these depressions represented the internal uplift of the Cordillera Frontal, the regional arc volcanism and the initial exhumation of the Precordillera. The provenance changes recorded in the detrital zircon ages

suggested an initial shortening in the Frontal Cordillera in coincidence with the change of an eolian to fluvial sedimentation in the adjacent foreland basin during the Early Miocene (24–17 Ma). Levina et al. (2014) considered the probable age of exhumation induced by the shortening and rise of the Precordillera to be between 12 and 9 Ma.

Furthermore, several authors (Japas, 1998; Ré et al., 2001; Japas et al., 2002; Cortés et al., 2005, 2006; Oriolo et al., 2015, among others) divided Precordillera into two segments: northern and southern, as a consequence of the reactivation of NW, WNW and NE trending structures. These authors have suggested that these cross-strike structures are reactivated pre-Neogene fabrics, although not discarding a possible Miocene age.

2.2 Local Geology

Detailed mapping of the study area allowed the identification of several geological units (Figure 1c). From the oldest to the most recent, the stratigraphic units are (1) Cambrian–Ordovician sedimentary rocks, mainly consisting of limestones, dolomites, and shales; (2) Silurian–Devonian greywackes and shales of marine origin; (3) Neogene sedimentary rocks (conglomerates, sandstones and shales); (4) Quaternary colluvial–alluvial consolidated deposits and (5) unconsolidated modern deposits (gravel, sand, silt and clay) in the piedmont and river channels (Milana et al., 1993; Ramos and Vujovich 2000, Perucca et al. 2012, Levina et al., 2014; Perucca et al., 2015).

The Neogene deposits are present in the central portion of the valley with an estimated thickness of 1000 m. Levina et al. (2014) described clastic depositional patterns in these intermountain exposures of Central Precordillera assigned to the Late Oligocene-Miocene retroarc foreland basin system. The oldest strata recorded a transition at ~24 Ma from ephemeral playa lake/incipient dune field conditions to a regional eolian system. About 17

Myr ago, the eolian system replaced a fine-grained floodplain deposition. Upward coarsening fluvial and alluvial fan deposits reflect a 17–8 Ma shift from distal to proximal foreland basin facies, locally influenced by synorogenic volcanic activity. However, in the study area, most apatite (U-Th)/He ages fall in 12 Ma (Levina et al., 2014). These authors pointed out that this pattern is consistent with an eastward (cratonward) progression of thin-skinned thrusting and resultant structural fragmentation of the foreland basin into isolated intermountain segments. Neogene rocks outcrops in the central-south portion of the Gualilán-La Cantera tectonic depression are characterised by fine and coarse sandstones to fine conglomerates trending N-S and dipping between 20° to 50° near the west-dipping La Cantera Fault, delineating a westward-dipping homoclinal structure that would have generated the tilt of the entire Neogene basin. Quaternary alluvial deposits composed of coarse-grained loose sandy-gravel layers with an average total thickness of approximately 1–3 m (Perucca et al., 2012, 2015) cover the Neogene rocks.

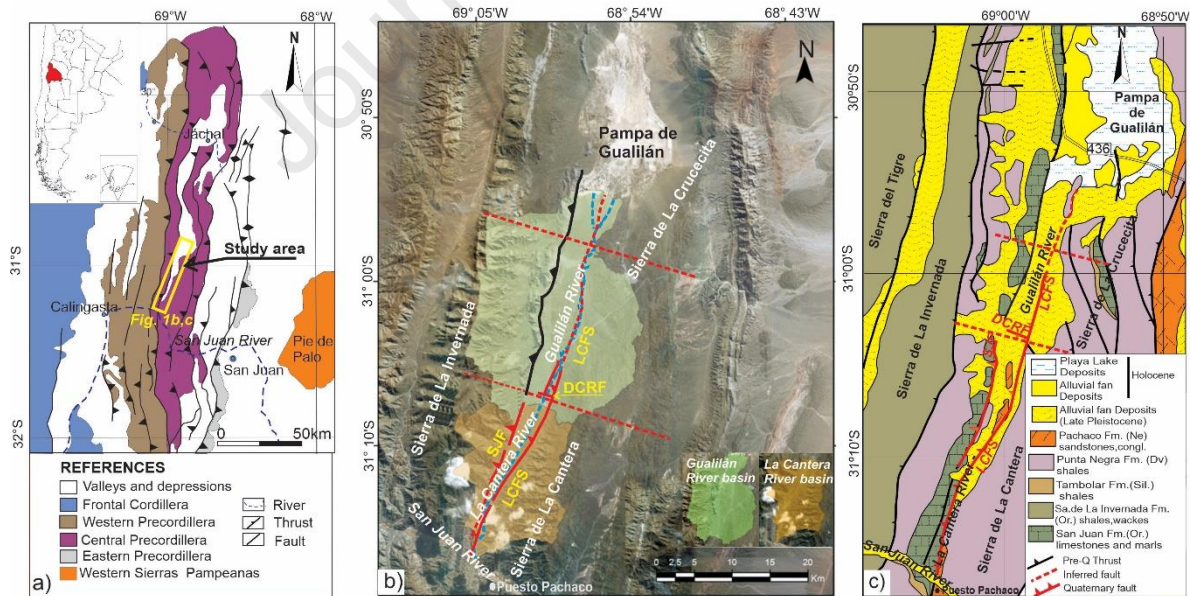


Figure 1. a) Location of the study area in the province of San Juan, Argentina; b) Satellite image with the Gualilán-La Cantera River basins location and main fault sections with evidence of late Pleistocene-Holocene tectonic activity. SJF: San Juan Fault, LCFS: La

Cantera Fault System, DCRF: Divisadero Coba Rubia Fault, c) Geological sketch map and location of the main active faults and NW lineaments along the intermountain Gualilán-La Cantera Valley in the Precordillera area (Modified from Vargas et al., 2020).

2.3 Neotectonics

Most active structures in the study area are related to compressional faulting, but earthquakes on these active reverse faults are not always accompanied by surface ruptures (Siame et al. 2006).

In the Gualilán and La Cantera river valley piedmonts, faults with evidence of Quaternary tectonic activity are present. They are reverse faults that trend N-S to NNE, with eastern vergence, consistent with the structural style of the Central Precordillera (Figure 2a-d).

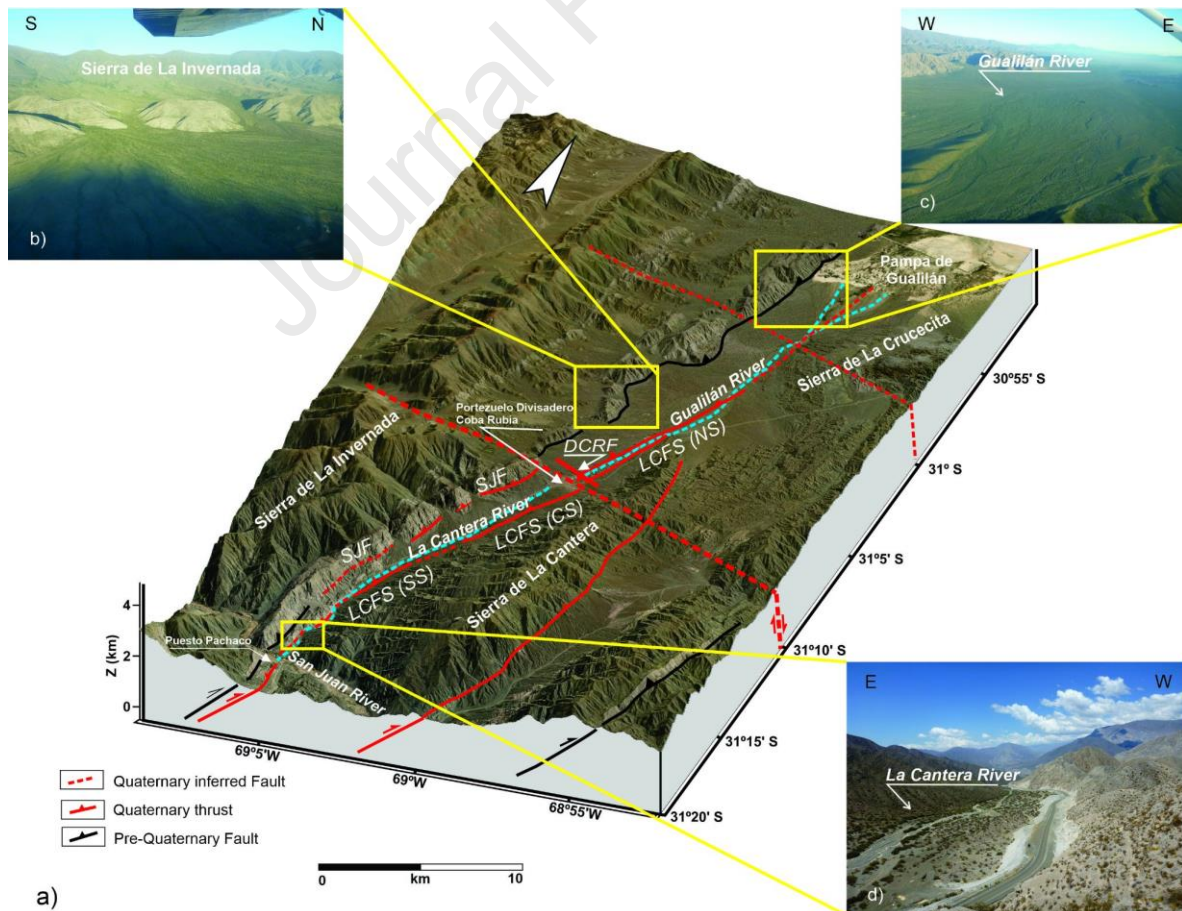


Figure 2. a) Digital Elevation Model (DEM) and satellite image (ASTER GDEM) of the Gualilán-La Cantera river valleys showing its topographic features and location of the main Quaternary structures, La Cantera Fault System (LCFS), north section (NS), central section (CS) and south section (SS), San Juan Fault (SJF) and Divisadero Coba Rubia Fault (DCRF). Yellow boxes show: b) Oblique aerial view to the west of Sierra de La Invernada morphostructural unit, c) Aerial view to the north of the wide Gualilán River valley, d) Aerial view to the south of the narrow La Cantera River valley.

San Juan Fault (SJF)

There are very scarce antecedents referring to the tectonic activity of this structure. Mingorance (1998) mentioned an east-vergent thrust affecting the eastern topographic front of the Sierra de La Invernada. The fault trends ~N-S in its northern section, NE to the south, and dips to the west with unknown angles (Figure 2). Their recurrence intervals and slip rates are also unknown, as suggested by Casa et al. (2014).

La Cantera Fault System (LCFS)

The La Cantera Fault System (LCFS) is considered one of the most active structures in the Central Precordillera of San Juan (Perucca et al. 2014a, b; 2015). This fault system extends for ~47 km along the Gualilán-La Cantera intermountain valley with an average trend of 20°E. Three main sections (27 km long) could be recognized in the western piedmont of the Sierra de La Cantera: North, Central and South, defined by a series of landforms as simple and compound counter slope fault scarps, staircased alluvial terraces, sag ponds, flexural scarps, aligned springs, broom-shaped drainage patterns, river diversions, beheaded channels, changes in incision depths, sinuosity and river gradient (Perucca et al., 2014a, b; 2015) (Figure 2). However, LCFS has not yielded conclusive geomorphological evidence of its northward continuation up to the latitude of the Pampa de Gualilán.

Fault sections dip at angles varying between 15° and 30° W in the Northern section, to approximately 40° W in the Central section (Figure 4c, d), and up to 60° W in the Southern section (Perucca et al, 2014a).

LCFS is an out-of-sequence fault (Cristallini, 1998), where the uppermost portion of the Ordovician carbonates (San Juan Formation) constitutes the base of the imbricate sequence. In the central section of the fault system, Perucca et al. (2015) described two outcrops where Ordovician limestones thrust onto Neogene deposits and Quaternary alluvial levels. However, on the surface, this fault primarily affects Neogene and Holocene to recent alluvium deposits in the western piedmont of the Sierra de La Cantera. To the south, the fault trace borders the eastern flank of the Sierra de La Invernada (Figure 2).

Perucca et al. (2014a, b, 2015) studied four fault exposures along the LCFS to assess their kinematics and other characteristics. Data were gathered from metric scale outcrops located along river cuts. In all of the natural trenches, the east-verging faults trend between 150° to 190° azimuth and dip 10° to 60° to the west. Quaternary alluvial sediments affected by faults were dated using the AMS method, indicating Holocene tectonic activity, which was traced to mid- to Late-Holocene soil levels (4580 ± 50 BP to 1576 to 1423 Cal years BP) and early to mid-Holocene alluvial terraces (11962 to 11615 Cal years BP to 4865 to 4830 Cal years BP) (Perucca et al., 2015). These authors suggested that the LCFS accommodates a recurrent interval of at least 2000 ± 500 yrs, that is, multiple events (at least four earthquakes) during the last 11000 years (Perucca et al., 2015).

3. Methodology

3.1 Structural and geomorphological analysis

Structural and geomorphological analyses were performed using topographic data, fieldwork, and digital satellite imagery (Landsat 7-TM and SPOT 5). Also, three swath averaged topographic profiles were built (0.5 km window), two across the valley (W-E) and the other in a N-S direction in coincidence with the two major river collectors of the depression. The mean, maximum and minimum elevations of the used DEM (ALOS PALSAR-12.5 m) were projected into cross-section planes. The strip width was set to 0.5 km with a length of ~14, 17, and 48 km to examine trends in slope and local relief at this scale of observation. Orthogonal (W-E) swath profiles crossing the Gualilán and the La Cantera valleys were selected to represent the asymmetry of the ranges, the main morphostructural units, the differences in their heights, slopes and extension, and the influence of faults. Data processing of ALOS PALSAR DEM (12.5 m resolution) was carried out using ArcGIS software to highlight the main topographic characteristics of the valley.

In addition, fieldwork observations carried out in a natural trench located on the right bank of the Gualilán River allow us to address the Coba Rubia fault kinematics.

3.2 Data and gravity anomalies

Regional and local gravity anomalies were used to investigate the mass-density distribution of the Earth's interior and provide constraints on the geological structures of the subsurface from crustal to upper mantle depths. The regional geophysical datasets were derived from the World Gravity Map 2012 (WGM 2012), a 1-minute resolution digital grid computed from the EGM2008 gravity geopotential model and the ETOPO 1 global relief model (Balmino et al., 2011). EGM2008 was obtained through the processing of terrestrial, marine, and aerial measurements, satellite altimetry, and satellite gravimetry (GRACE mission). It was developed by the National Agency of Geospatial Intelligence (NGAI) in spherical harmonics up to degree and order 2160 degrees (Pavlis et al., 2008). ETOPO 1 is an Earth's topography–

bathymetry data set up to degree and order 10800 (Amante and Eakins, 2009). Based on rigorous geodetic and geophysical computations (Balmino et al., 2012), WGM provides spherical free air, Bouguer, and isostatic gravity anomalies that account for the gravity contribution of most surface masses.

For local scale gravimetric analysis, two N-S detailed gravity profiles were measured to analyze local gravity anomalies associated with the main oblique structures: a western profile, >45 km long, and an eastern one, ~6 km long. In addition, a detailed W-E profile, ~7 km long, was measured in the northern portion of the Gualilán Valley to recognize the northward continuation of the La Cantera Fault System. These detailed gravity profiles provide local coverage to interpolate subsurface density variations with high spatial stability without mathematical approximation errors.

We measured the gravity profiles with gravity stations at ~500 m intervals and a precision of 0.05 mGal. We used a SCINTREX CG-5 automated gravity meter (#40484), and gravity stations were georeferenced using GPS leveling. Gravity anomalies were calculated using the standard methods (e.g., Hinze et al., 2013). The theoretical gravity is according to the Somigliana expression for the Geodetic Reference Ellipsoid. The vertical gravity gradient for the free-air correction is $FAC=0.3086 h$, and the simple Bouguer correction is an infinite slab of h thickness and $2,67 \text{ g/cm}^3$ upper crust density (Hinze, 2003). The complete Bouguer anomaly is the difference between the observed gravity and the corrected theoretical gravity and more accurately removes the effects of terrain. Terrain corrections were computed using the Kane (1962) and Nagy (1966) algorithms taking into account local (10 m x 10 m) and regional (100 m x 100 m) elevation models. Local and regional elevation data were obtained from the Shuttle Radar Topography Mission (SRTM) global model (Farr et al., 2007).

4. Results

4.1 Swath profiles analysis

We drew up two W-E cross-section swath profiles across the valley (North and South) and the third with a N-S trend, to highlight the most distinctive topographic features of the depression (Figure 3a). The northern profile shows a broad valley ranging from about 17 km to 10 km in width with the most significant elevation difference between the Sierra de La Crucecita to the east (~2000 m asl) and the Sierra de La Invernada to the west (~3500 m asl). The Sierra de La Invernada has an extensive piedmont (~7 km) with an average slope of about 48%, showing wide alluvial fans with low incisions towards the distal portion, which increase towards the steep mountainous front of the calcareous hills. The eastern flank of these very elongated hills is affected by a west-dipping reverse fault. By contrast, the western piedmont of the Sierra de La Crucecita is very narrow (300-2500 m) with slopes close to 5%, showing several alluvial levels (Figure 3b). The alluvial plain of the Gualilán River lies on the eastern portion of the valley.

The southern profile shows that the topographic difference between both mountain ranges decreases. The Sierra de La Crucecita does not exceed 3000 m asl in this sector, whereas the Sierra de La Invernada has an elevation of ~3700 m asl. Both piedmonts have a similar extension and slope (~10%), and the La Cantera River is located symmetrically in the central portion of the valley (Figure 3c). At these segments, the valley width is less than 2 km and turns narrower further south reaching only 400 m next to the San Juan River. The N-S profile shows that along the Gualilán River, there are no major variations in the local relief, and the maximum and minimum topography have similar values. Only in its headwater variations become more evident, close to the W-E structure located at the Portezuelo Divisadero Coba Rubia (Figure 3d). This is the only section of the river showing strath terraces, suggesting a

larger river incision. The highest point in the profile (Divisadero Coba Rubia) is the water divide between both river basins, coincident with an E-W ($\sim 110^\circ$ azimuth) lineament (Figure 3d). The longitudinal profile of the Gualilán River is slightly concave, indicating that it has not yet reached an equilibrium stage. Besides, the swath profile of the La Cantera River is notoriously convex. It shows fluvial incisions near the water divide and also in the lower section close to its mouth in the San Juan River, where unpaired fill terraces were identified, four on its right margin and only one on the left. Both sectors are related to the LCFS (Vargas et al., 2020).

The average slope of the La Cantera River is 4.7%, higher than that of the Gualilán River (1.8%). In the La Cantera River basin, the height difference between the highest point of the headwaters in the portezuelo (2182 m) and the San Juan River (1188 m) is 994 m. For the Gualilán River basin, the difference between the head (2182 m) and the mouth of the river in Pampa de Gualilán (1621 m) is only 561 m. The swath profiles allow the identification of several areas with river incisions.

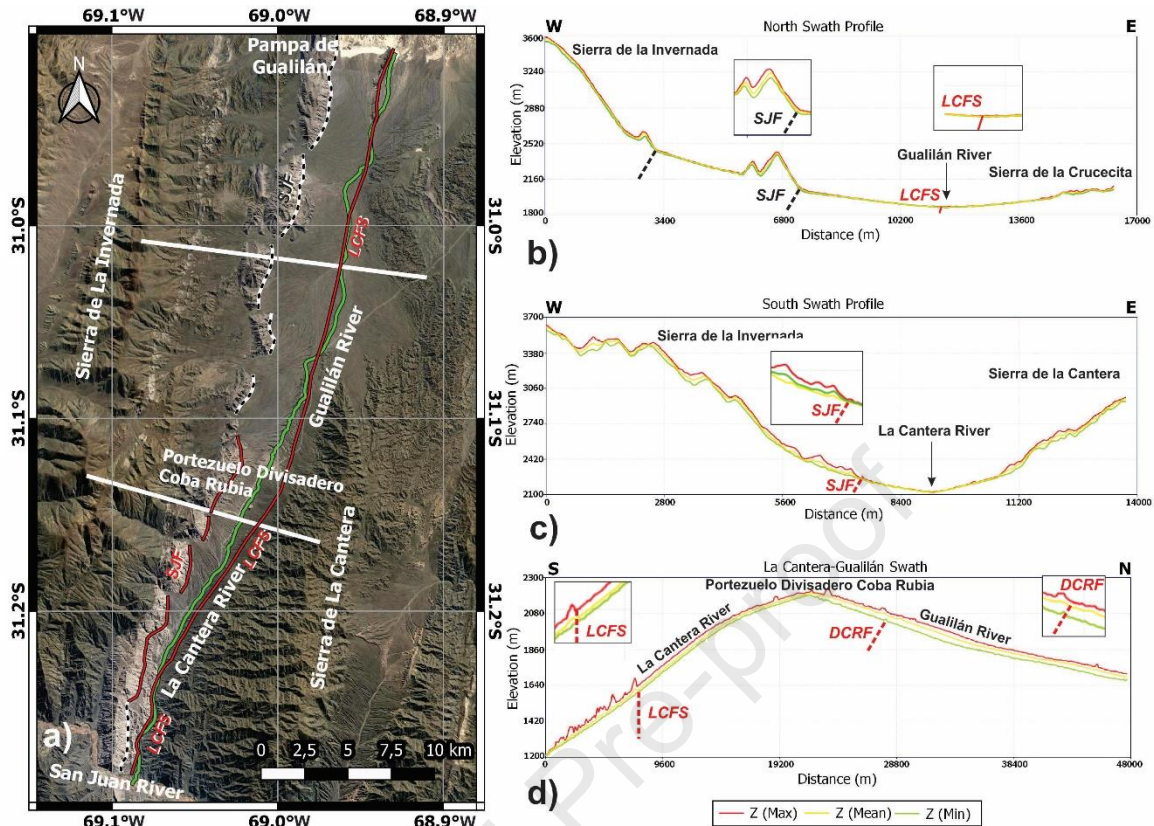


Figure 3. a). Satellite image of the Gualilán-La Cantera valley and location of the swath profiles. Each profile shows focal statistics of the highest, mean and lowest elevation, respectively (with 0.5 km window), b) North cross profile (W-E), c) South cross profile, and d) La Cantera-Gualilán longitudinal N-S profile. LCFS (La Cantera Fault System), SJF (San Juan Fault), DCRF (Divisadero Coba Rubia Fault).

4.2 Neotectonic analysis

In addition to the structures and natural exposures already described in previous works (e.g., Mingorance, 1998; Millán and Perucca, 2011; Perucca et al., 2014a, b; 2015, among others), we present new in situ observations of several morphotectonic features located in both piedmonts along the Gualilán-La Cantera depression.

Several parallel fault scarps related to the San Juan Fault are arranged along the eastern border and piedmont of the La Invernada orographic system, overlapping Paleozoic rocks over Neogene to Quaternary sediments (Figure 4a, b). Furthermore, these N-S faults seem to affect progressively younger deposits to the east.

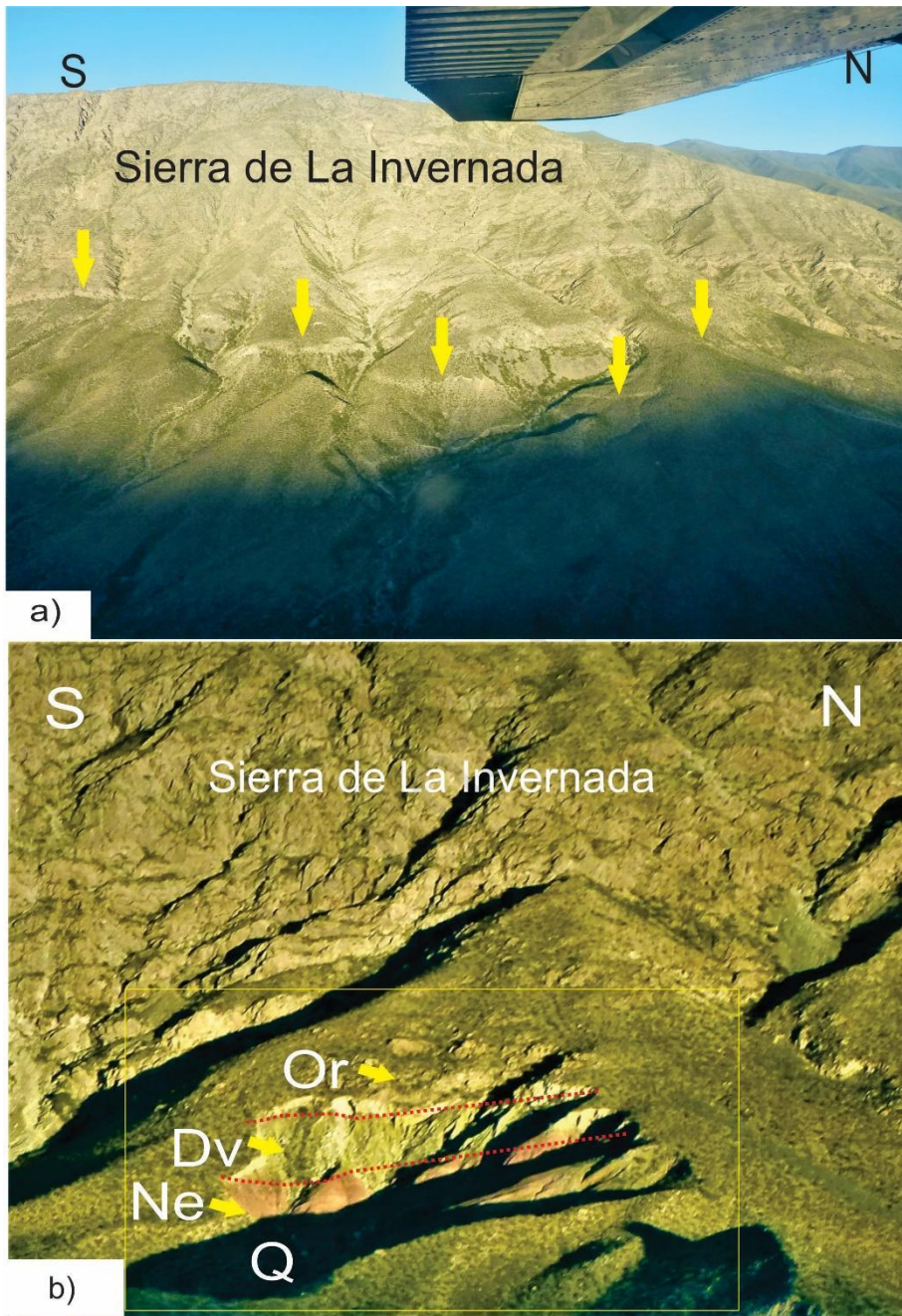


Figure 4. a) Oblique aerial view to the west of the San Juan fault (Eastern flank of the Sierra de La Invernada), yellow arrows show several favor-slope scarps, developed in basement rocks, pre-Quaternary, and/or Quaternary alluvial deposits, b) Yellow arrows point the inferred fault traces (red dotted lines): Ordovician limestones (Or) thrusting Devonian sandstones (Dv) and these to Neogene sandstones (Ne)-Quaternary deposits (Q).

In the right margin of the Gualilán River ($31^{\circ} 07'S - 69^{\circ}W$), a natural exposure in a strath terrace shows deformation associated with two sub-parallel faults (Figure 5a) called in this work Divisadero Coba Rubia Fault (DCRF). These north-verging reverse faults put Oligocene-Miocene sedimentary rocks over Quaternary alluvial gravels. The fault planes do not cut the surface, but two gentle flexures of the terrace top coincide with the brittle deformation displayed in the outcrop. The oldest exposed unit (Ne) corresponds to pink Neogene sandstones and siltstones of unknown base and a maximum exposed thickness of 2 m. These rocks are partly overlaid by angular gravel-dominated (wackes and limestones) and carbonate-cemented alluvial deposits assigned to the Late Pleistocene-Holocene (Figure 5a). The faults, trending W-E and dipping 40° - 46° to the south respectively, affect the Neogene unit (Ne) and the alluvial deposits (Pl-H) with vertical offsets ranging from 10 to 30 cm (Figures 5b, c, d). Slickensides measurements in both fault planes (Az 130° , pitch 20° and 44°) indicate an oblique-slip (dextral) reverse main component (Figure 5b, c). DCRF faults seem to flatten toward the surface, separating blocks of approximately equal dip, producing a positive flower-like structure. Associated with these faults, minor centimetric palm-tree (positive flower-like) structures were observed (Figure 5e).

DCRF faults could be related to an oblique structure coincident with the headwaters of the La Cantera (flows to the south) and Gualilán (flows to the north) river basins, as was mentioned by Vargas et al. (2020) (Figure 6a, b). These authors pointed to a high gradient of the La Cantera River and a considerable drop in elevation between the headwaters and the outlet of the La Cantera River regarding the Gualilán River, with slight unevenness and gentler slopes.

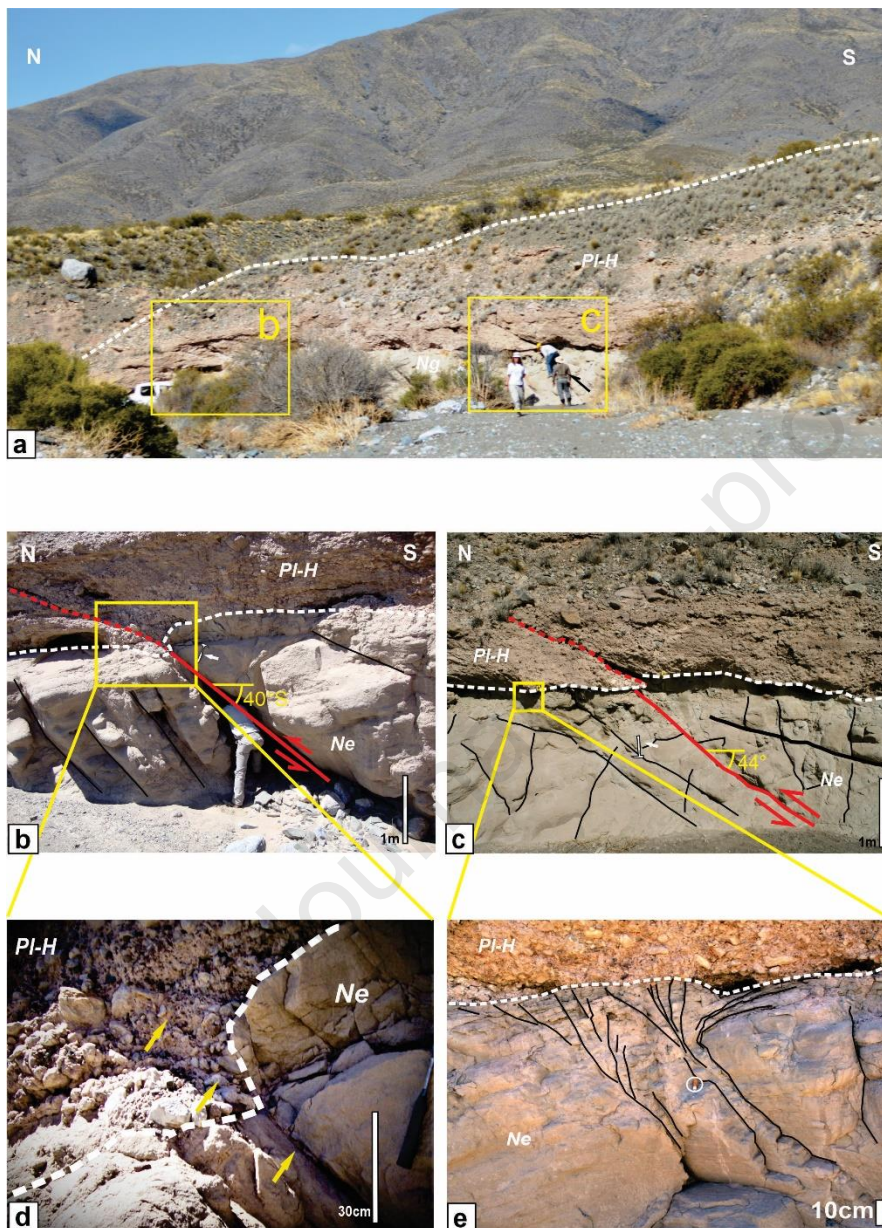


Figure 5. a) View to the east of a natural exposure in a strath terrace on the right margin of the Gualilán River. The reverse faults dipping to the south place Neogene rocks over alluvial deposits assigned to the Late Pleistocene-Holocene. Yellow rectangles point figures b and c; b) Exposure of a reverse fault dipping 40° S. The yellow rectangle shows fault detail of figure d; c) Exposure of a reverse fault dipping 44° S, the yellow rectangle shows positive flower-like structures detail of Figure e; d) and e) Detail photographs of structures shown in b (Yellow arrows indicate the fault plane, and the dotted line point the contact between the

Neogene rocks and the Quaternary alluvial deposits) and c (Little white circle shows a lips protector as scale) respectively.

The most remarkable morphological evidence corresponds to the main trace of the LCFS. However, regarding this structure, its northern continuation is not clear. Although the morphotectonic features are very noticeable in the central and southern portion of the Gualilán-La Cantera river valley, to the north, the evidence is very subtle. For example, the Gualilán drainage network shows a N-S control, the alluvial levels coming from Sierra de La Invernada have anomalous slopes (tilted to the west) and east-vergence Ordovician limestones and Devonian sandstones and siltstones outcrop forming elongated hills with a N-S trend (Figures 6a-d).

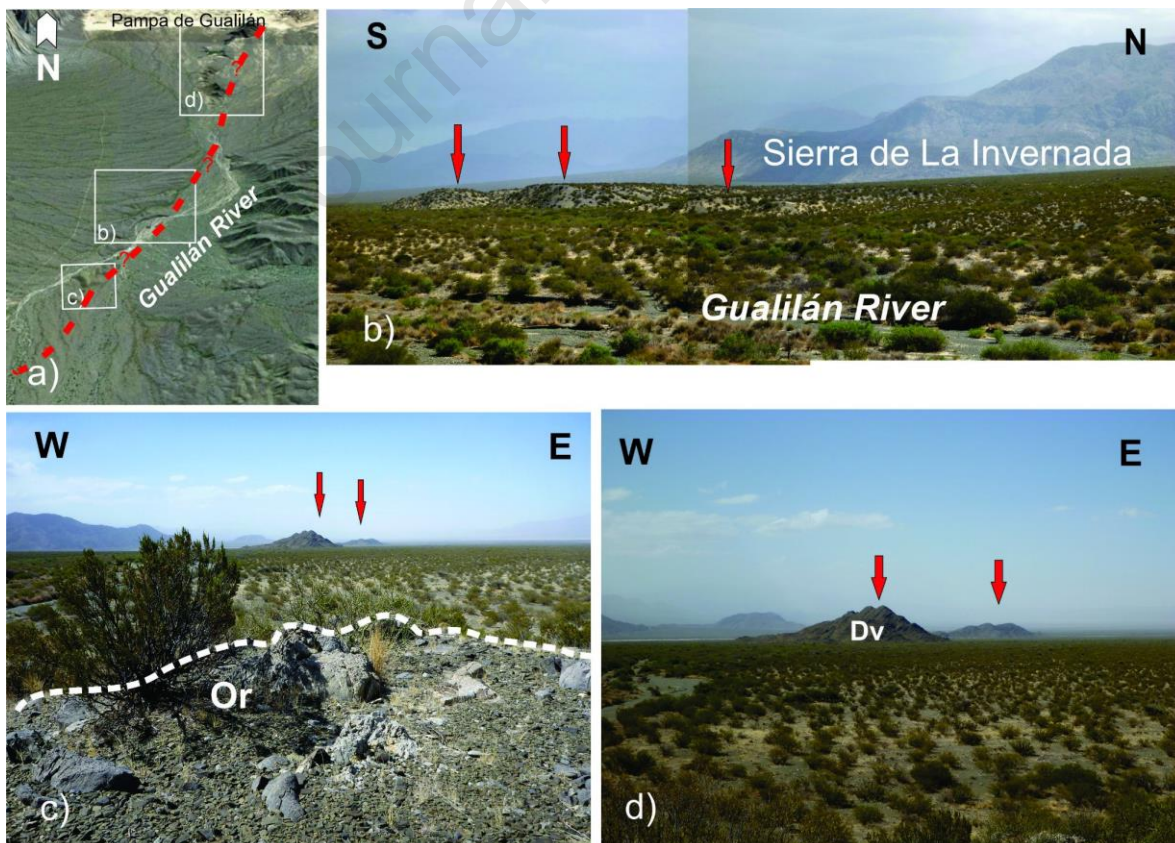


Figure 6. a) Satellite image showing the location of pictures taken in the field, in red dotted line, the inferred La Cantera fault trace, b) View to the southwest showing Sierra de La Invernada raised alluvial levels anomalously tilted to the west (red arrows), c) North view: In the foreground is an outcrop of brecciated Ordovician limestones (white dotted line) and, in the background, elongated Devonian hills trending N-S (red arrows).d) East-vergent Devonian hills trending N-S (red arrows) in the middle portion of the Gualilán alluvial plain.

4.3 Gravity data analysis

Regional gravity analysis

The anomaly charts obtained for the Gualilán-La Cantera Valley reflect high-density contrasts at crustal and lithospheric scales, where positive and negative values would be associated with the different geological units exposed in the valley. Changes in gravity anomaly patterns suggest a strong correlation between regional structures and the gravity influence of the Andean root. The free-air anomaly chart (Figure 7a) shows a good correspondence with the topographic features exposed along the La Cantera Valley and the thrust fronts that uplift the mountain ranges of Central Precordillera, that is, the Sierra de La Invernada to the west and the Sierra de La Crucecita-La Cantera to the east. The high gravity gradient indicates a boundary well defined by N-S thrusts uplifting these parallel mountain ranges and the intermountain depression Gualilán-La Cantera. Furthermore, the relative maximum and minimum gravity anomalies associated with the uplifted and depressed areas appear to be controlled by these N-S thrusts, which dominated the landscape evolution during the Andean cycle.

The topographic correction (Figure 7b) is supplementary, taking into account the gravitational effect of the ground roughness, where the highest values are usually associated with the increase in terrain irregularities. In the study area, the highest values of topographic correction are located in the Divisadero Coba Rubia area (6 to 8 mGal) and in the mountain

ranges that limit the depression, such as Sierra de La Cantera and Sierra de La Crucecita (12 to 15 mGal). On the other hand, the minimum values are located in the southeast portion of the Pampa de Gualilán (1 to 2 mGal), where the terrain is flat or gentler.

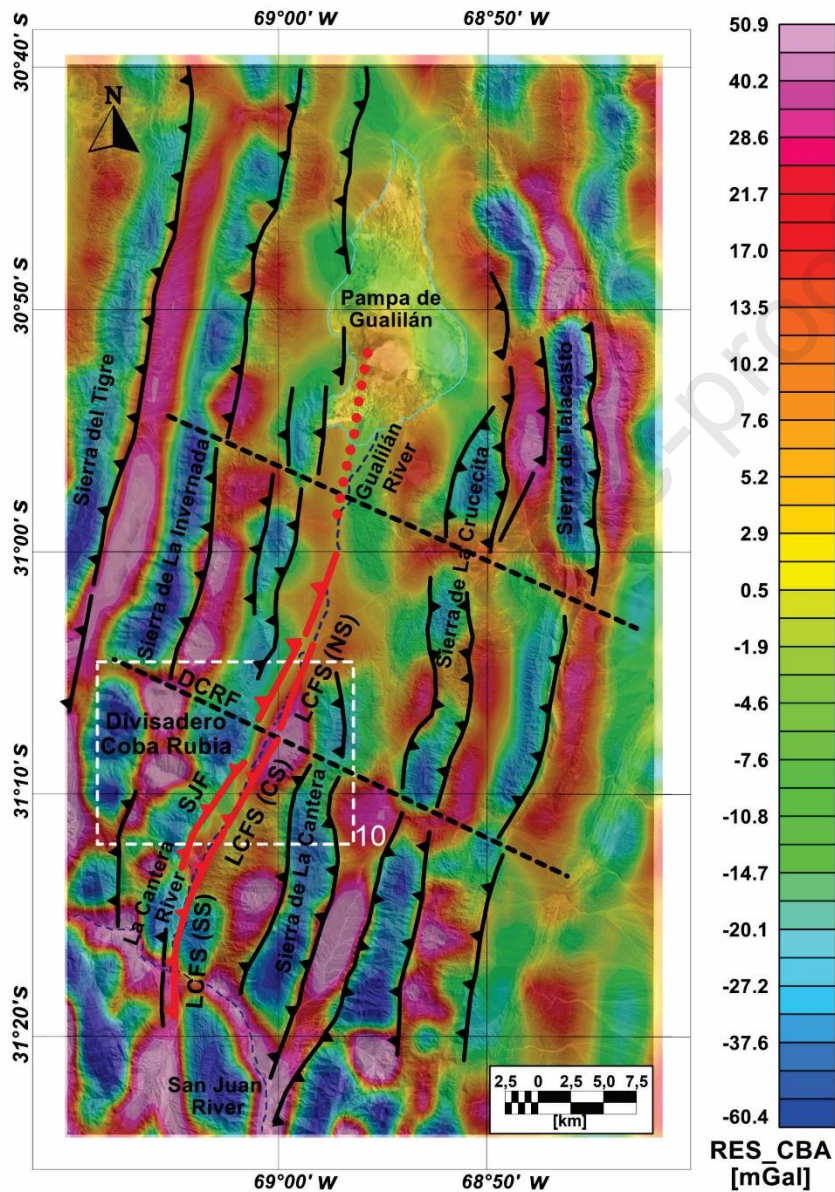


Figure 7. a) Free-air gravity anomaly chart, b) Terrain correction chart. In black lines, pre-Quaternary faults, in red lines Quaternary faults, LCFS: La Cantera Fault System; SJF: San Juan Fault; DCRF: Divisadero Coba Rubia Fault. The red dotted line indicates the inferred continuation to the north of LCFS, and the black dotted lines show the main NW lineaments.

The complete Bouguer anomaly chart (Figure 8a) shows negative values which can be associated with Precordillera ranges like Sierra de La Crucecita-La Cantera and Sierra de La Invernada. Also, positive values prevail on longitudinal (N-S) intermountain tectonic valleys as the La Cantera-Gualilán depression, which shows a NW lateral gravity contrast bounding Precordillera ranges and valleys. Maximum gravity values are observed in the Portezuelo Divisadero Coba Rubia area.

The isostatic anomaly chart (Figure 8b) shows non-zero values both in elevated and depressed zones of the study area. It would suggest that the crust is unbalanced according to a simple isostatic Airy system. Allmendinger et al. (1990) and Alvarado et al. (2009) pointed out that this region could be an example of the dynamic sustentation associated with high buoyancy and the flat slab geometry of the Nazca plate related to Juan Fernández ridge subduction.

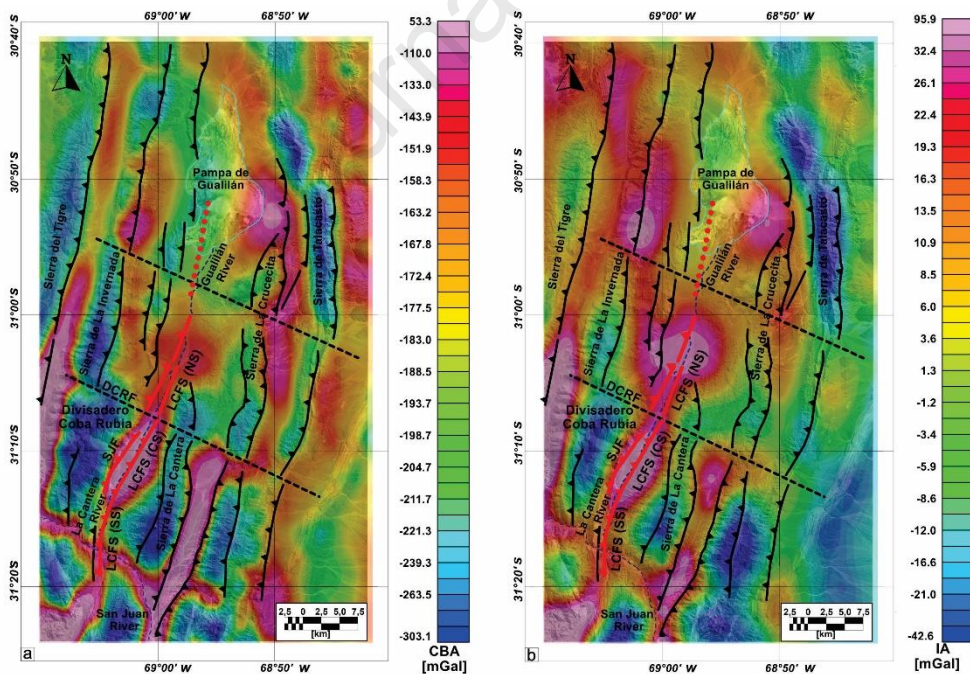


Figure 8. a) Complete Bouguer anomaly chart, b) Isostatic anomaly chart. In black lines, pre-Quaternary faults, in red lines Quaternary faults, LCFS: La Cantera Fault System; SJF: San

Juan Fault; DCRF: Divisadero Coba Rubia Fault. The red dotted line indicates the inferred continuation to the north of LCFSs, and the black dotted lines show the main NW lineaments.

Since the study herein presented deals with shallow geological structures, a bandpass filtering technique (Hinze et al., 2013) was applied to gravity anomalies. Due to the powerful influence of the Andean root on the west, a bandpass filter rejecting all wavelengths higher than 15 km and lower than 3 km proved to be the most efficient filter to separate the regional and residual components of the complete Bouguer anomaly. The residual anomaly chart (Figure 9) enhances the responses of the relatively shallow causative geological units (mostly short-wavelength anomalies) and attenuates the deeper crustal gravity effects (long-wavelength anomalies). Besides, very short wavelengths were also low pass filtered to improve the signal/noise ratio. The residual anomaly chart shows relative gravity maxima associated with the uplifted morphostructural units of Precordillera and relative minima related to the intermountain valleys. The N-S trending structures, like the San Juan Fault in the eastern flank of Sierra de La Invernada, are easily identifiable on the chart as they bound the east and west of the intermountain valleys filled by Neogene to Quaternary deposits (Pampa de Gualilán and Gualilán-La Cantera rivers Valley). It is also possible to identify a density contrast coincident with the Gualilán River alluvial plain, suggesting the continuation of the LCFS northward to the Pampa de Gualilán as a blind/buried thrust. Besides, the residual anomaly chart reveals north-south lateral density contrasts associated with NW to W-E structures that would segment the Precordillera and the intermountain valleys into several depocenters separated from each other by basement highs (Figure 9).

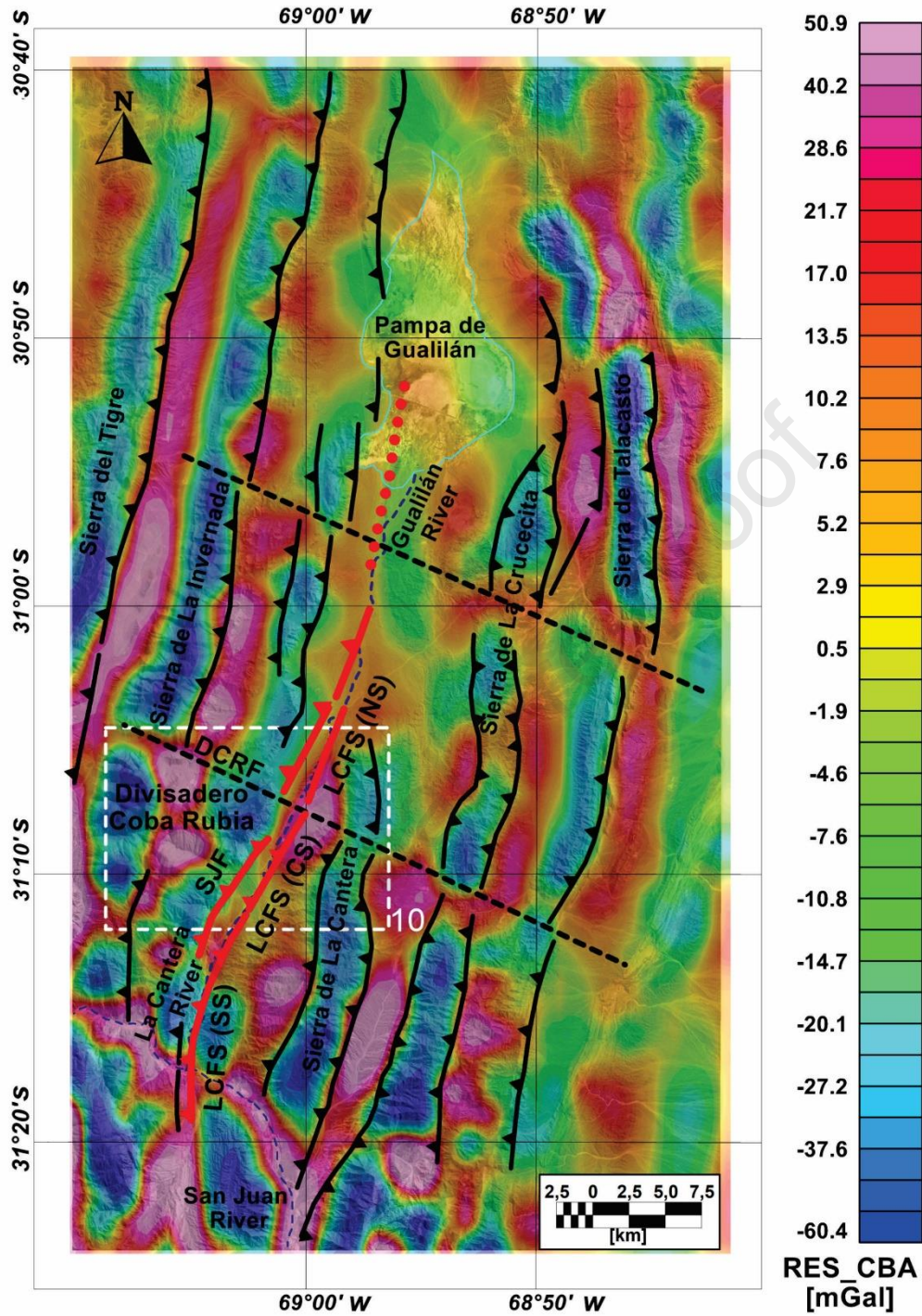


Figure 9: Residual complete Bouguer anomaly chart. In black lines, pre-Quaternary faults, in red lines are the Quaternary faults, LCFS: La Cantera Fault System; SJF: San Juan Fault; DCRF: Divisadero Coba Rubia Fault. The red dotted line indicates the inferred continuation to the north of LCFS, and the black dotted lines show the main NW structures. The white dashed line box in figure b shows the location of figure 10.

Full zooms were made of the complete Bouguer and residual Bouguer anomaly charts (figures 8a and 9) to enhance the NW structures and intra-basement highs in the Divisadero Coba Rubia area; (figures 8a and 9) the resulting anomaly charts are shown in figures 10 a,b. Figures 10 c, d detail the relationships between Complete Bouguer and Residual Bouguer anomaly charts and the N-S and NW-trending structures that control deformation in the Divisadero Coba Rubia area.

These Complete Bouguer anomaly charts show a good correlation between the topographic highs and the La Cantera and Gualilan water divide, coincident with the -120 mGal isoanomaly. On the other hand, the maximum relative values for the Complete Bouguer anomaly are observed to the south of the Divisadero Coba Rubia area. In these areas, it is possible to observe values ranging from -120 mGal to -60 mGal for the Complete Bouguer anomaly and from 0 mGal to 30 mGal for the Residual anomaly. Geologically, these relative gravity maximums would correspond to limestone outcrops which would be surface evidence of N-S thrust fold systems, which are coincident with the 30 mGal isoanomaly, as long as the San Juan fault coincides with the 0 mGal isoanomaly.

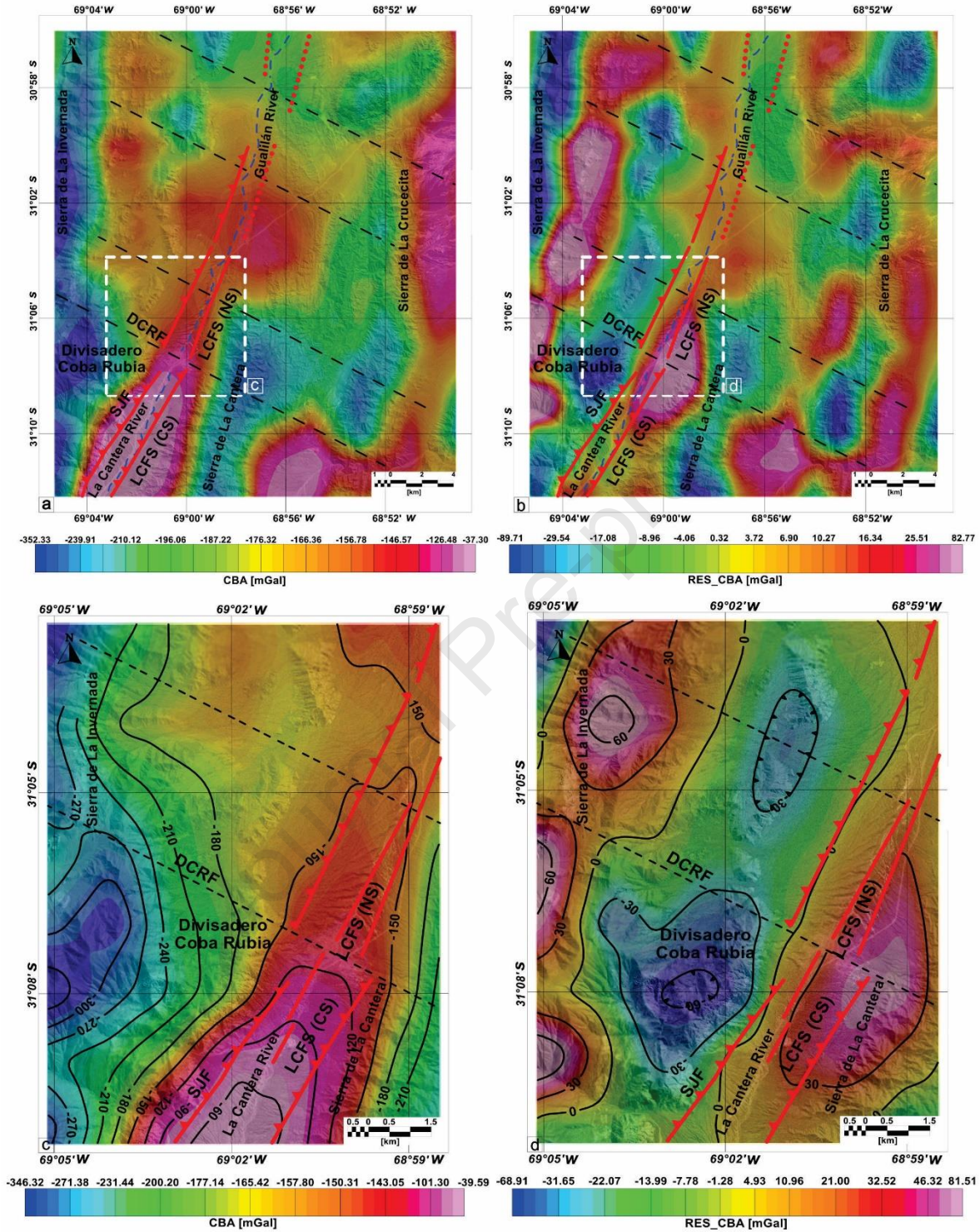


Figure 10 a) Complete Bouguer anomaly chart, b) Residual Bouguer anomaly chart, white dotted line boxes show figures c) and d) with zoomed areas suggesting the existence of topographic highs consistently with the gravity isoanomalies. In red lines Quaternary thrusts, LCFS: La Cantera Fault System, CS: Central Section, NS: North Section; SJF: San Juan Fault; DCRF: Divisadero Coba Rubia Fault. The black dotted lines show the main NW lineaments.

Local gravity analysis

The local gravity analysis was based on two N-S (A-A' to the west and C-C' to the east) and one W-E (B-B') Complete Bouguer anomaly profiles along the Gualilán-La Cantera river valley (Figure 11).

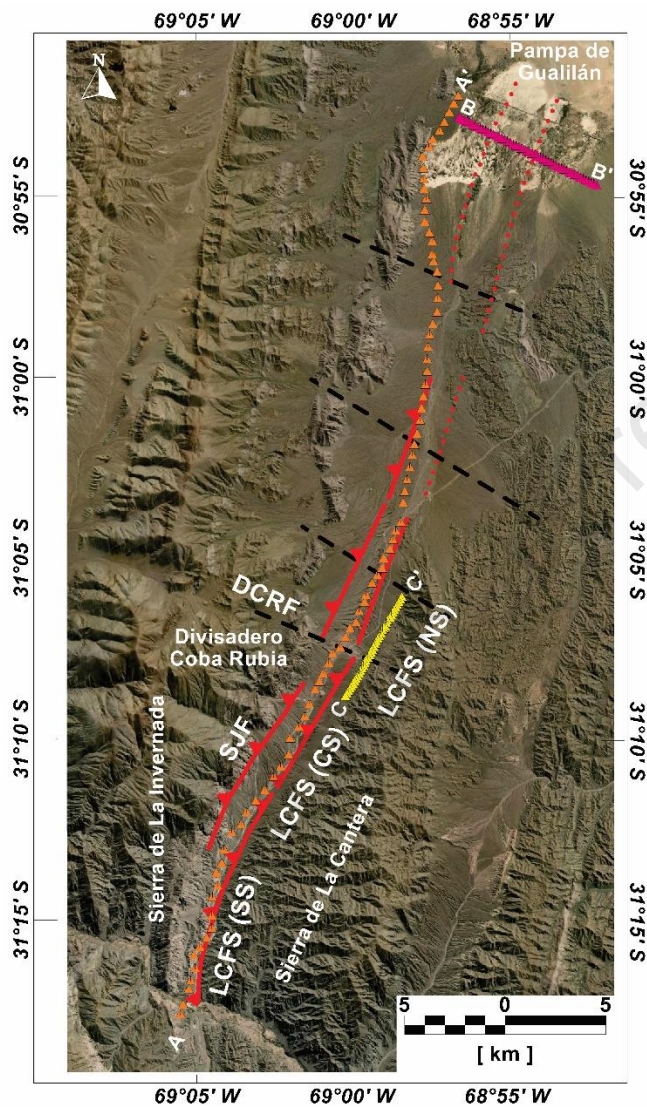


Figure 11. Satellite image with the location of detailed gravimetric profiles A-A' (orange), B-B' (pink) and C-C' (yellow) and main Quaternary structures location: Divisadero Coba Rubia Fault (DCRF); La Cantera Fault System (LCFS), Southern Section (SS), Central Section (CS) and Northern Section (NS) and San Juan Fault (SJF). The red dotted lines indicate the inferred Quaternary faults. The black dotted lines show the main NW lineaments.

The western gravity profile (A-A') shows an increase in the topography-corrected Bouguer anomaly values observed from north to south (Figure 12). We interpret that these changes in the Complete Bouguer anomaly values suggest the existence of a set of segmented N-S trending depocenters with Neogene-Quaternary sedimentary infill. These depocenters seem to be delimited by buried blocks limited by NW oblique structures. In the central portion of the Gualilán-La Cantera Valley, and related to the Divisadero Coba Rubia fault, it is possible to appreciate subtle changes in the gravity gradients, from 61 to 58 mGal, coincident with the water divide between the Gualilán and La Cantera river basins (Figure 12). In agreement with the observed changes in the A-A' profile, the eastern (C-C') profile shows local variations in the anomaly values in the N-S direction (Figure 12). These changes would also be related to the Divisadero Coba Rubia fault, which is consistent with the W-E lateral continuity of this structure. Towards the southern portion of the La Cantera river valley, maximum gravity anomaly values seem to be associated with the gravimetric response of the basement deposits (Ordovician limestones) and the thin Quaternary alluvial fill. On the other hand, the B-B' profile crosses the northern portion of the Gualilán river in a W-E direction. It shows anomalous values related to the density contrast between the Devonian basement and the alluvial fill of the valley (Figure 12). This contrast in density between the early Paleozoic and Quaternary deposits would be consistent with a northward continuation of the LCFS as a blind/covered structure.

Regarding the residual anomalies analysis (Figure 13), the chart shows a good correspondence with the values obtained for the complete Bouguer anomalies (Figure 12). In the western N-S profile (A-A'), a set of depocenters that segment the Gualilán-La Cantera valley could be related to the NW structures, with a marked change in the gradient inflections in the Divisadero Coba Rubia area. The eastern N-S profile (C-C') is consistent with the A-A' profile since it also would reflect the existence of a NW structure that segments the depression into two main basins. In the W-E direction, variations in the gravity values suggest the contact between the depocenter basal units and the Quaternary alluvial infill. On the other hand, the B-B' profile north of the Gualilán depression shows variations in the gravity gradients from W to E, interpreted as the La Cantera Fault continuity as a blind structure.

In addition, based on the gravity anomaly we have identified three structures with N20°E to N25°E azimuth, which segment the Pampa de Gualilán area, where the gravity residual

responses are the result of the overlapping of Paleozoic units (Ordovician-Devonian rocks) over Neogene and Quaternary deposits by the La Cantera Fault System.

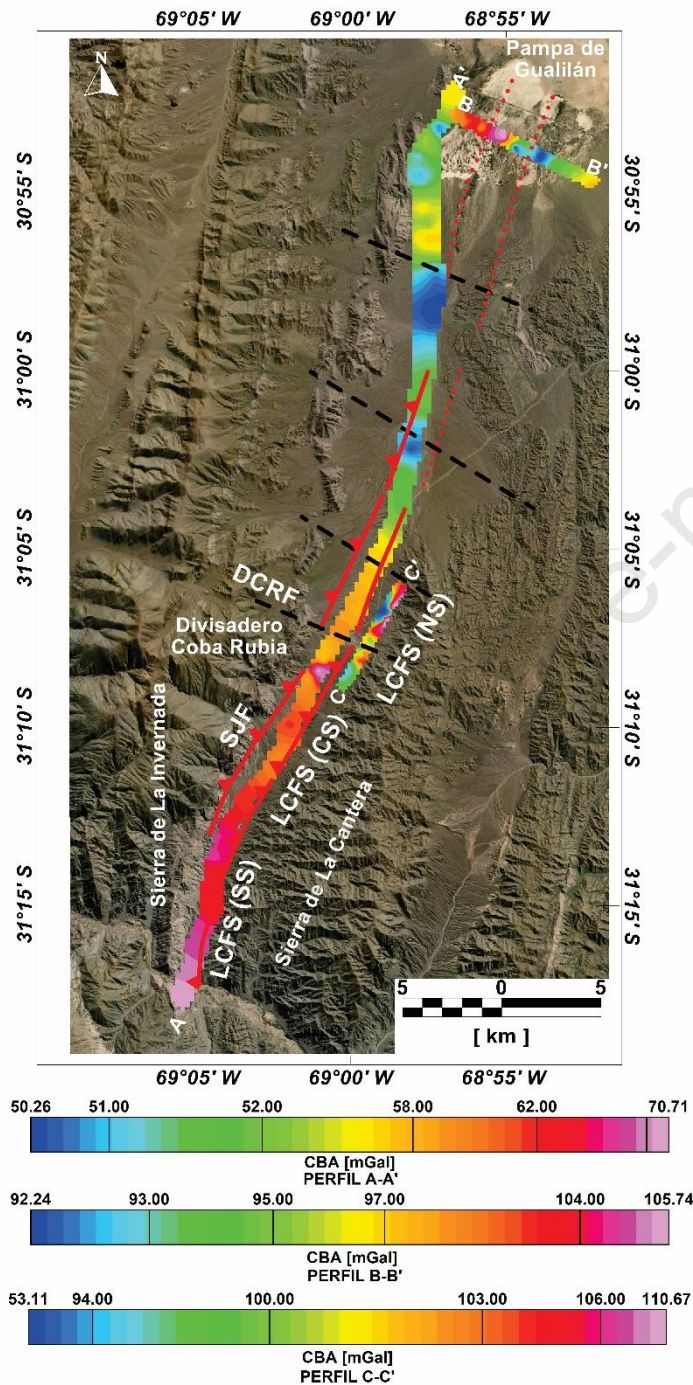


Figure 12. Local Complete Bouguer anomaly profile and main Quaternary structures identified in the Gualilán-La Cantera valley: Divisadero Coba Rubia Fault (DCRF); La Cantera Fault System (LCFS), Southern Section (SS), Central Section (CS) and Northern Section (NS) and San Juan Fault (SJF) and main NW lineaments (black dotted lines).

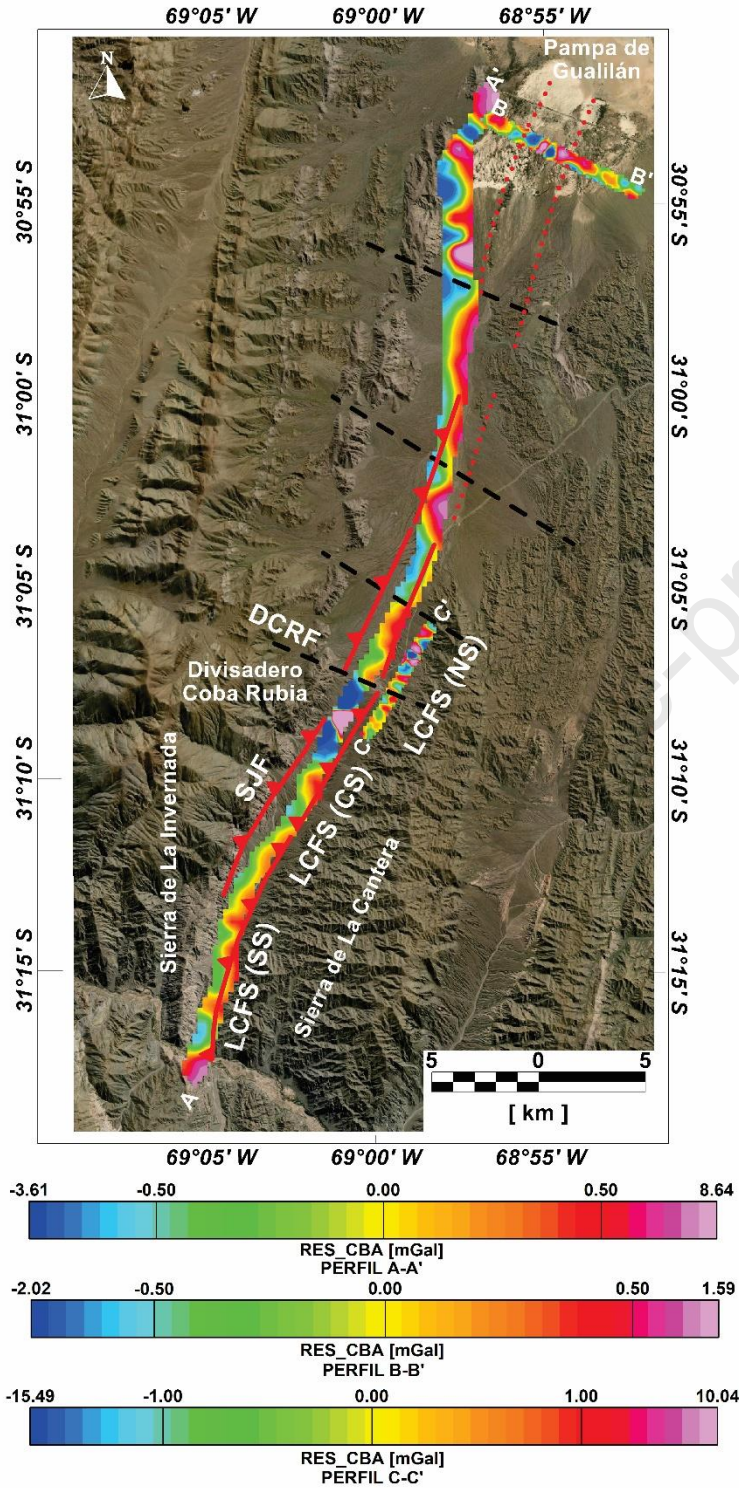


Figure 13. Residual Complete Bouguer anomaly profile and main Quaternary structures identified in the Gualilán-La Cantera valley. Divisadero Coba Rubia Fault (DCRF); La Cantera Fault System (LCFS), Southern Section (SS), Central Section (CS) and Northern Section (NS) and San Juan Fault (SJF), and main NW lineaments (black dotted lines).

5. Discussion

In the present analysis, evidence of Late Pleistocene to Holocene tectonic activity was identified in the Gualilán-La Cantera depression, consistent with the fold-and-thrust belt style of Central Precordillera. The San Juan fault, located in the eastern flank of Sierra de La Invernada, is a N-S east-vergence thrust that puts Ordovician limestones onto Neogene to Quaternary deposits. Although detailed features along this fault trace are not visible, it seems to be the same Precordilleran neotectonic pattern of the LCFS. The LCFS provides remarkable surface evidence of Late Pleistocene-Holocene tectonic activity along the western piedmont of the Sierra de La Cantera (Perucca et al., 2015). However, there was no reliable evidence of the continuation of this structure in the northern portion of the Gualilán-La Cantera depression.

Also, orthogonal transpressive W-E faults, called in this work Divisadero Coba Rubia, dip to the south segment of the N-S longitudinal valley. Morphotectonic analysis (Vargas et al., 2020) and field evidence reveal that the Quaternary activity and topographic relief of the water divide between Gualilán and La Cantera river basins could be controlled by oblique transpressive faults which have formed a pop-up-like structure, transferring displacement between two thrust faults (LCFS and SJF).

The W-E swath profiles show notable variations along latitude. The north profile shows a big difference in height (~1600 m) between the Sierra de La Invernada and Sierra de la Crucecita. Also, the eastern piedmont of the Sierra de La Invernada is more extensive than the western piedmont of the Sierra de La Crucecita, giving place to a strongly asymmetric valley where the main collector (N-S) is displaced towards the east. However, south of the structure named Divisadero Coba Rubia the valley is symmetric and both piedmonts have a similar extension.

The N-S swath profile shows the longitudinal profile of the Gualilán and La Cantera rivers and their water divide. It is possible to observe a convex and non-steady-state river profile for the La Cantera River as was suggested by Vargas et al. (2020). By contrast, the Gualilán River has a slightly concave profile, with a gentle slope and a greater length, indicating a river in a state of equilibrium. In addition, the gravity analysis has allowed us to better identify and characterize the surface and the subsurface geology providing information about the arrangement of the blind or buried structures.

The gravity anomaly charts derived from WGM 1.0 global maps show marked changes in horizontal gradients, in terms of the observed anomaly values between the high morphostructural units that constitute Precordillera and the depressed intermountain morphostructural units. Sharp gravity contrast has an elongated shape in the N-S direction that could be related to the N-S trending LCFS, in coincidence with the Gualilán River channel suggesting a blind thrust to the north axis of the valley. Besides, the anomaly charts analysis allowed us to interpret the existence of two main buried structural highs trending NW and several minor NE lineaments segmenting and controlling the Gualilán-La Cantera rivers depression. From the detailed gravity N-S profile, a set of NW and NE structures that limit and control valleys are recognized. From west to east, the gravity anomalies could correspond to N-S faults that uplift the Precordillera mountain ranges. Also, from north to south, they are consistent with the two rivers that drain the Gualilán-La Cantera valley, suggesting at least two depocenters disconnected from each other by a basement high. Thus, the Gualilán river basin, located in the northern sector of the valley, flows to the north to the Pampa de Gualilán, separated by a structural high from that of the La Cantera River, which drains to the south as a tributary of the San Juan River. These structural highs that segment

the depression seem to have a direct correlation with the set of NW and NE oriented structures that could accommodate the deformation associated with the Andean tectonic regime.

Several studies (Ré et al., 2001; Japas et al., 2002; Ré and Japas, 2004; Oriolo et al., 2013; 2015; Perucca and Ruiz, 2014; Alcacer et al., 2020a, b) described NW and NE oblique transpressional and transtensional mega-zones crossing the Precordillera fold-and-thrust belt. Japas et al. (2015) suggested that the Central Precordillera domain is characterized by a heterogeneous vertical axis rotation pattern linked to the first stage of deformation lately overprinted by localized anticlockwise rotation. This configuration was induced by NNW-trending sinistral transpressional belts. Also, Oriolo et al. (2015) described WNW and NW structures reactivated as sinistral strike-slip or sinistral transpressional structures that do not develop unless they represent inherited structures. These authors inferred that these structures postdate regional N-S thrusting.

Alcacer et al. (2020a) pointed out that changes in gravity gradients observed in the anomalies charts would suggest the existence of NW cross-strike structures segmenting Eastern Precordillera (Sierra de Villicum) and Sierras Pampeanas Occidentales (Sierra Pie de Palo). Also, Alcacer et al. (2020b) interpreted from a geophysical and morphotectonic analysis, the existence of two main buried structural highs segmenting the Iglesia Valley (between Cordillera Frontal and Precordillera), one of them trending NW and the other ~ W-E.

From the regional and detailed geophysical analysis, natural exposures and swath profiles interpretation, we suggest that there is a structural segmentation of the Gualilán-La Cantera valley controlled by NW and NE structures crossing the depression. These oblique structures could have played a significant role in controlling tectonic block rotations during the Neogene. Thus, the gravity response of the basement and the two river basins of the tectonic

valley show a close relationship with the surface and subsurface structures associated with the development of these opposite river basins.

It is well known that several areas in the Central Andes of South America are situated on sedimentary basins or foreland fold-thrust belts that are bordered by, contain, or are underlain by active buried N-S-trending thrust faults and NE or NW-trending strike slip oblique structures (Japas et al., 2002, 2015; Oriolo et al., 2013, 2015). These buried/blind faults are poorly studied and so, estimating their seismic potential is difficult due to the shortage of on-fault geologic or geomorphic evidence from past earthquakes (Burrato et al., 2012). Stein and Yeats (1989) pointed “large earthquakes can take place not only on faults that cut the Earth’s surface but also on 'blind' faults under folded terrain” and so, potentially hazardous and unrecognized buried faults generating large-magnitude hidden earthquakes pose a serious threat to millions of people in many parts of the world (Berberian, 1995). As a local example, the most recent earthquakes that occurred in the San Juan Province, such as the 1944 (Mw 7), 1952 (M 6.8), 1977 (7.4) and 2021 (Mw 6.4) events, did not have a clear associated surface rupture (Siame et al., 2015; Meigs and Nabelek, 2010, Perucca and Vargas, 2014, Ammirati et al., 2022), suggesting that the hazard posed by blind and hard-to-identify faults is a critical issue. Two of these events (1952 and 2021 earthquakes), appear to be associated with blind or covered strike slip oblique structures. Alvarado and Beck (2006) pointed out that the 1952 earthquake showed a focal mechanism consistent with a NE-striking active oblique fault with left-lateral neotectonic displacement. In addition, Ammirati et al. (2022), suggested a depth solution for the 2021 earthquake in coincidence with a NE-striking, NW-dipping basement fault defined by the zone of high seismic activity beneath the Precordillera. In these sense, these authors do not exclude a coseismic activation of the oblique emergent structures that could be expected during future large earthquakes.

Conclusions

Neotectonic deformation analyses require the use of complex methodologies including geomorphology, geology, and geophysics. Identified subsurface structures have to be crosschecked by surface geologic or morphotectonic information to validate the neotectonic age of deformation.

Therefore, a morphotectonic, neotectonic and gravimetric analysis in the N-S Gualilán-La Cantera Valley, located between the Sierra de La Crucecita-La Cantera to the east and the Sierra de La Invernada to the west was performed. In this depression, new evidence of Late Pleistocene to Holocene tectonic activity was identified. As well as the N-S east-vergence Quaternary structures and the NW lineaments, two W-E and north-vergence oblique structures were identified, named Divisadero Coba Rubia Fault. The analysis of these neotectonic structures, the residual gravity anomalies chart and the north-south gravity profile suggest the existence of two main NW buried structures, the southern one reflected by the water divide between the Gualilán and La Cantera river basins. Also, a set of NE and SE secondary lineaments seems to control the valley topography limiting depocenters from the structural highs. In this way, the gravity data analyzed in the Gualilán-La Cantera river valley allowed us to identify the deep structures of the region and their relationship to the geological outcrop and the evolution of the opposite river basins. Also, the length of the LCFS may be longer than previously estimated in the western piedmont of the Sierra de La Cantera, as farther north of the northern section there is gravimetric evidence in support of a blind continuation, in coincidence with the valley axis, towards the Pampa de Gualilán depocenter.

The strong correlation between the gravity anomalies with the N-S and W-E neotectonic structures that segment the valley could imply the Andean reactivation of regional pre-Quaternary structures. These structures could continue as a control of deformation, segmentation and accommodation of the Andean fold and thrust belt.

In this work, gravimetric analysis is considered a fundamental tool for recognizing surface and subsurface structures controlling the Quaternary landscape. This study confirms some faults already recognized or suspected by fieldwork, and it also detects new faults masked in the surface, providing information on major fault depths and the relationship between different structures. Even though the neotectonic activity of such structures is difficult to assess because of the scarcity of surface ruptures, we propose them as potential seismogenic sources. Thus, they should not be underestimated, especially since these faults are located near four important dams along the San Juan River and some major cities of central-western Argentina.

Acknowledgements

The authors acknowledge funding from PID CICITCA 2018-19 (Universidad Nacional de San Juan), PID 013 CONICET, PICT 2016/0995 FONCYT and IPGH (GEOF 02-18) for supporting this research project.

References

Alcacer Sánchez, J., Rothis, M., Haro, F., Perucca, L., Miranda, S., Vargas, N., 2020a. Geophysical analysis in a Quaternary compressive environment controlling the emplacement of travertine, eastern piedmont of Argentine Precordillera. *Journal of South American Earth Sciences*, 98, 102432. <https://doi.org/10.1016/j.jsames.2019.102432>

Alcacer Sánchez, J., Tejada, F., Rothis, M., Perucca, L., Haro, F., Miranda, S., 2020b. El método potencial (gravimetría) como herramienta en el análisis morfotectónico del valle de Iglesia, provincia de San Juan. *Geología del Cuaternario. Revista de la Asociación Geológica Argentina*, 71, 62-78.

Allmendinger, R., Figueroa, D., Zinder, E., Beer, J., Mpodozis, C., Isacks, B. L., 1990. Foreland shortening and crustal balancing in the Andes at 30° latitude. *Tectonics*, 9, 789-809.

Alonso J.L., Rodríguez Fernández L.R., García-Sansegundo J., Heredia N., Farías P., Gallastegui J., 2005. Gondwanic and Andean structure in the Argentine Central Precordillera: The Río San Juan section revisited. 6th International Symposium on Andean Geodynamics. IRD Editions (Institut de Recherche pour le Développement), Extended Abstracts, Paris, 36-39.

Alvarado P, Beck S., 2006. Source characterization of the San Juan (Argentina) crustal earthquakes of 15 January 1944 (MW 7.0) and 11 June 1952 (MW 6.8) *Earth Planetary and Science Letters*, 243,615–631.

Alvarado, P., Pardo, M., Gilbert, H., Miranda, S., Anderson, M., Saez, M., Beck, S., 2009. Flat slab subduction and crustal models for the seismically active Sierras Pampeanas region of Argentina. In *Backbone of the Americas: Shallow subduction, plateau uplift, and ridge and terrane collision*. Editors S. M. Kay, V. A. Ramos, and W. R. Dickinson (Boulder, CO: Geological Society of America Memoir), 204, 261–278. doi:10.1130/2009.1204(12)

Amante, C., Eakins, B.W., 2009. ETOPO1: 1 arc-minute global relief model: procedures, data sources and analysis. NOAA Tech. Mem. NESDIS NGDC24, Boulder(Co).

Ammirati, J., Mackaman-Lofland, C., Zeckra, M., Gobron, K., 2022. Stress transmission along mid-crustal faults highlighted by the 2021 Mw 6.5 San Juan (Argentina) earthquake. *Science Report*, 12(1), 17939. doi: 10.1038/s41598-022-22752-6.

Audemard, F.A., Perucca, L., Pantano, A., Avila, C., Onorato, M., Vargas, H., Alvarado, P., Viète, H., 2016. Holocene compression in the Acequión valley (Andes Precordillera, San Juan Province, Argentina): geomorphic, tectonic, and paleoseismic evidence. *Journal of South American Earth Sciences*, 67, 140-157.

Balmino, G., Vales, N., Bonvalot, S., A. Briais, 2012. Spherical harmonic modelling to ultra-high degree of Bouguer and isostatic anomalies. *Journal of Geodesy*, 86, 499–520.

Berberian, M. 1995. Master "blind" thrust faults hidden under the Zagros folds: active basement tectonics and surface morphotectonics. *Tectonophysics*, 241, 193-224.

Burrato, P., Vannoli, P., Fracassi, U., Basili, R., Valensise, G., 2012. Is blind faulting truly invisible? Tectonic-controlled drainage evolution in the epicentral area of the May 2012, Emilia-Romagna earthquake sequence (northern Italy). *Annals of geophysics = Annali di geofisica*, 55. 10.4401/ag-6182.

Cahill, T., Isacks, B.L., 1992. Seismicity and the shape of the subducted Nazca plate. *Journal of Geophysical Research*, 97, 17503–17529.

Casa, A., Yamín, M., Wright, E., Costa, C., Coppolecchia, M., Cegarra, M., 2011. Deformaciones Cuaternarias de la República Argentina, Sistema de Información Geográfica: Instituto de Geología y Recursos Minerales, Servicio Geológico Minero Argentino, Publicación 171, v1.0 DVD, Buenos Aires.

Casa, A., Yamín, M., Wright, E., Costa, C., Coppolecchia, M., Cegarra, M., Hongn, F., 2014. Deformaciones cuaternarias de la República. Argentina. Sistema de Información Geográfica. Instituto de Geología y Recursos Minerales. Servicio Geológico Minero Argentino, Publicación N°171, v.1.0 DVD. Buenos Aires.

Cortés, J.M., Pasini, M., Yamín, M., 2005. Paleotectonic controls on the distribution of Quaternary deformation in the southern Precordillera, Central Andes (31°30'–33° sl). In

International Symposium on Andean Geodynamics, 6, Extended Abstracts, 186-189. Barcelona.

Cortés, J.M., Casa, A., Pasini, M., Yamín, M., Terrizzano, C.M., 2006. Fajas oblicuas de deformación neotectónica en Precordillera y Cordillera Frontal (31°30'-33°30' ls): controles paleotectónicos. *Revista de la Asociación Geológica Argentina*. 61 (4), 639-646.

Costa, C., Machette, M.N., Dart, R.L., Bastías, H.E., Paredes, J., Perucca, L., Tello, G., Haller, K.M., 2000. Map and database of Quaternary faults and folds in Argentina. U.S. Geological Survey Open-File Report 00-0108, 81pp.

Cristallini, E.O., 1998. Introducción a las fajas plegadas y corridas. I. Las fajas plegadas y corridas (Unpublished), 4-92.

Cristallini, E.O., Ramos, V.A., 2000. Thick-skinned and thin-skinned thrusting in the La Ramada fold and thrust belt: crustal evolution of the High Andes of San Juan, Argentina (32° SL). *Tectonophysics*, 317, 205-235.

Farr, T.G., Rosen, P.A., Caro, E., Crippen, R., Duren, R., Hensley, S., Kobrick, M., Paller, M., Rodríguez, E., Roth, L., Seal, D., Shaer, S., Shimada, J., Umland, J., Werner, M., Oskin, M., Burbank, D., Alsdorf, D., 2007. The shuttle radar topography mission. *Reviews of Geophysics* 45 (2). RG2004, doi: 10.1029/2005RG000183.

Furque, G., González, P., Caballé, M., 1998. Descripción de la hoja geológica 3169-II, San José de Jáchal (Provincias de San Juan y La Rioja). Servicio Geológico y Minero Argentino 259, 150 pp. Buenos Aires.

Hinze, W.J., 2003. Bouguer reduction Density-Why 2.67? *Geophysics*, 68, 1559-1560.

Hinze, W. J., R. R. B. Von Frese, A. H. Saad, 2013. Gravity and Magnetic Exploration. Cambridge University Press (Verlag), 525 pp.

Hofmann-Wellenhof, B., Moritz, H., 2006. *Physical Geodesy*. 2. Vienna. Springer Vienna, 403pp.

Japas, M.S., 1998. Aporte del análisis de fábrica deformacional al estudio de la faja orogénica andina. Homenaje al Dr. Arturo J. Amos. *Revista de la Asociación Geológica Argentina*, 53, 15.

Japas, M.S., Ré, G.H., Barredo, S.P., 2002. Lineamientos andinos oblicuos (entre 22° y 33°S): definidos a partir de fábricas tectónicas. I. Fábrica deformacional y de sismicidad. In *Congreso Geológico Argentino*, 15, 326-331. El Calafate.

Japas, M.S., Ré, G.H., Oriolo, S., Vilas, J., 2015. Palaeomagnetic data from the Precordillera fold and thrust belt constraining Neogene foreland evolution of the Pampean flat-slab segment (Central Andes, Argentina). In: Pueyo, E. L., Cifelli, F., Sussman, A. J., Oliva-Urcia, B. (eds) *Palaeomagnetism in Fold and Thrust Belts: New Perspectives*. Geological Society, London, Special Publications, 425. <http://doi.org/10.1144/SP425.9>

Jordan, T.E., Allmendinger, R.W., Brewer, J.A., Ramos, V.A., Ando, C.J., 1983. Andean tectonics related to geometry of subducted Nazca plate. *Geological Society of America Bulletin*, 94, 341-361.

Jordan, T.E., Allmendinger, R.W., Damanti, J.F., Drake, R.E., 1993. Chronology of motion in a complex thrust belt: The Precordillera. *Journal of Geology*, 101, 135-156.

Kane, M.F., 1962. A Comprehensive System of Terrain Corrections Using a Digital Computer. *Geophysics*, 27, 4, 455-462.

Levina, M., Horton, B., Fuentes, F., Stockli, D., 2014. Cenozoic sedimentation and exhumation of the foreland basin system preserved in the Precordillera thrust belt (31–32° S), southern central Andes, Argentina. *Tectonics*, 33, 1659-1680, doi: 10.1002/2013TC003424.

Mc. Calpin, J., Rockwell, T., Welldon II, R., 2009. Paleoseismology of Strike-Slip Tectonic Environments. In: McCalpin J (2nd. edition) Paleoseismology. Academic Press, USA, 613pp.

Meigs, A., Nabelek, J., 2010. Crustal-scale pure shear foreland deformation of western Argentina. *Geophysical Research Letters*, 37 L11304, 5. doi:10.1029/2010GL043220.

Milana, J.P., Cevallos, M., Zavattieri, A., Prampano, M., Papu, H., 1993. La secuencia terciaria de Pachaco: sedimentológica, edad, correlaciones y significado paleogeográfico, *in* 12° Congreso Geológico Argentino and 2° Congreso de Exploración de Hidrocarburos, 1, 226-234.

Millán, J.L., Perucca, L., 2011. Análisis neotectónico del extremo norte del sobrecorrimiento La Cantera, provincia de San Juan, Argentina. *Revista Mexicana de Ciencias Geológicas*, 18, 337-348.

Mingorance, F., 1998, Evidencias de paleoterremotos en la falla activa La Cantera-Cinturón de empuje de la Precordillera, San Juan, Argentina: 10° Congreso Latinoamericano de Geología, II, 161-166.

Nagy, D., 1966. The Prism Method for Terrain Corrections Using Digital Computers. *Pure Applied Geophysics*, 63, 31-39.

Oriolo, S., Japas, M.S., Cristallini, E.O., Giménez, M., 2013. Cross-strike structures controlling magmatism emplacement in a flat-slab setting (Precordillera, Central Andes of Argentina). In *Deformation Structures and Processes within the Continental Crust* (Llana-Fúnez, S.; Marcos, A.; Bastida, F.; editors). Geological Society of London, Special Publications, 394. Doi: 10.144/ SP394.6. London.

Oriolo, S., Cristallini, E.O., Japas, M.S., Yagupsky, D., 2015. Neogene structure of the Andean Precordillera, Argentina: insights from analogue models. *Andean Geology*, 42, 20-35.

Onorato, M.R., 2013. Análisis Neotectónico del tramo sur de la Falla La Cantera, Precordillera de San Juan, Argentina. Trabajo Final de Licenciatura, Universidad Nacional de San Juan (Unpublished) San Juan, 82pp. Argentina.

Ortiz A., Zambrano J., 1981. La provincia geológica de Precordillera Oriental. Proceedings, 8° Congreso Geológico Argentino, San Luis, 3, 59-74.

Pacino, M., 2007. Absolute gravity measurements and gravity networks in south America *Nordic Journal of Surveying and Real Estate Research*, 4, 59-69.

Pavlis, N.K., Holmes, S.A., Kenyon, S.C., Factor, J.K., 2008. An Earth Gravitational Model to degree 2160: EGM2008. General Assembly of the European Geosciences Union, Vienna, Austria, 1, 13-18.

Perucca, L.P., Ruiz, F., 2014. New data on neotectonic contractional structures in Precordillera, south of Río de la Flecha: structural setting from gravity and magnetic data. San Juan, Argentina. *Journal of South America Earth and Sciences*, 50, 1-11.

Perucca, L., Vargas, H., 2014. Neotectónica de la provincia de San Juan, centro-oeste de Argentina. *Boletín de la Sociedad Geológica Mexicana*, 66, 291–304.

Perucca, L., Paredes, J., Tello, G., Bastías, H., 1999. Fallamiento activo en el área norte del sistema de fallamiento El Tigre, San Juan-La Rioja. *Revista de la Asociación Geológica Argentina*, 54, 206–214.

Perucca, L.P., Lara, G., Vargas, N., 2012. Nueva evidencia de actividad tectónica cuaternaria en la depresión Zonda-Maradona, provincia de San Juan. *Revista Asociación Geológica Argentina*, 69, 97-105.

Perucca, L., Rothis, M., Vargas, H., 2014a. Morphotectonic and neotectonic control on river pattern in the Sierra de La Cantera piedmont, Central Precordillera, province of San Juan, Argentina. *Geomorphology*, 204, 673-682.

Perucca, L., Onorato, M., Millán, J., Bustos, A., Vargas, H., 2014b. Variación del estilo de deformación a lo largo del sistema de falla La Cantera, Precordillera Central, San Juan, Argentina. *Revista de la Sociedad Geológica de España*, 27, 69-79.

Perucca, L., Rothis, M., Bezerra, F., Vargas, N., Lima, J., 2015. Late Quaternary evolution of the La Cantera Fault System (Central Precordillera, Argentina): a morphotectonic and paleoseismic analysis. *Tectonophysics*, 661, 200-209. doi: 10.1016/j.tecto.2015.08.041.

Ramos, V.A., 1988. The Tectonics of the Central Andes; 30° to 33° S latitude. *Geological Society of America Special Paper*, 218, 31-54.

Ramos, V.A., Vujovich, G.I., 2000. Hoja Geológica 3169-IV, San Juan, Provincia de San Juan. *Boletín* 243, Subsecretaría de Minería Nación, Servicio Geológico Minero Argentino, 82 pp. Buenos Aires.

Ramos, V.A., Cristallini, E.O., Pérez, D.J., 2002. The Pampean flat-slab of the Central Andes. *Journal of South American Earth Sciences*, 15, 59-78.

Ré, G.H., Japas, M.S., Barredo, S.P., 2001. Análisis de fábrica deformacional (AFD): el concepto fractal cualitativo aplicado a la definición de lineamientos cinemáticos neógenos en el noroeste argentino. *Revista de la Asociación Geológica Argentina, Publicación Especial*, 5, 75-82.

Ré, G.H., Japas, M.S., 2004. Andean oblique megashear zones: paleomagnetism contribution. *Geological Society of America Abstracts with Programs*, 36, Abstract 79033.

Rivas, C., Alcacer, J., Ortiz, G., Bilbao, I., Ammirati, J., Podesta, M., Alvarado, P., Perucca, L., Pérez, I., 2021. Crustal structure of the northern Andean Precordillera, Argentina, based on seismological and gravity data. *Journal of South American Earth Sciences*, 111, 103478, <https://doi.org/10.1016/j.jsames.2021.103478>.

Rojas Vera, E., Folguera, A., Zamora Valcarce, G., Gimenez, M., Ruiz, F., Martinez, M., Bottesi, G., Ramos, V., 2010. Neogene to Quaternary extensional reactivation of a fold and thrust belt: The Agrio belt in the Southern Central Andes and its relation to the Loncopué trough (38°–39°S). *Tectonophysics*, 492, 279-294. 10.1016/j.tecto.2010.06.019.

Siame, L.L., Bellier, O., Sebrier, M., 2006. Active tectonics in the Argentine Precordillera and western Sierras Pampeanas. *Revista de la Asociación Geológica Argentina*, 61, 604-619.

Siame, L.L., Sébrier, M., Bellier, O., Bourlès, D., Costa, C., Ahumada, E., Gardini, C., Cisneros, H., 2015. Active basement uplift of Sierra Pie de Palo (Northwestern Argentina): Rates and inception from ^{10}Be cosmogenic nuclide concentrations. *Tectonics*, 33, 1–25. doi:10.1002/2014TC003771

Stein, R. S., Yeats, R. S., 1989. Hidden Earthquakes. *Scientific American*, 260(6), 48–59. <http://www.jstor.org/stable/24987283>.

Suriano, J., Limarino, C.O., Tedesco, A.M., Alonso, M.S., 2015. Sedimentation model of piggyback basins: Cenozoic examples of San Juan Precordillera, Argentina: *GSL Special Publication*, 399, 221-244.

Tejada, F., Rothis, M., Onorato, M. R., Blanc, P. A., Perucca, L., Audemard-M., F. A., Vargas, N., 2021. Análisis neotectónico y paleosísmico de la falla Loma Negra Oriental, frente orogénico de la Precordillera Central, Argentina: *Boletín de la Sociedad Geológica Mexicana*, 73 (2), A080121. <http://dx.doi.org/10.18268/BSGM2021v73n2a080121>

Vargas, M., Rothlis, M., Esper-Angillieri, M.Y., Perucca, L. Vargas, N., 2020. Análisis morfométrico y morfotectónico de dos cuencas fluviales intermontanas colineales y opuestas de la Precordillera, Andes Centrales de Argentina: Boletín de la Sociedad Geológica Mexicana, 72, A111019. <http://dx.doi.org/10.18268/BSGM2020v72n1a111019n>

Whitney, R., Bastías, H., 1984. The Tigre fault of the San Juan Province, Argentina. The late Quaternary boundary of the Andes uplift: Geological Society of América Program with Abstract, 16, 6 - 693

Yáñez, G.A., Ranero, CR., von Huene, R., Díaz, J., 2001. Magnetic anomaly interpretation across the southern central Andes (32°-34° S): the role of the Juan Fernández Ridge in the late Tertiary evolution of the margin. Journal of Geophysical Research-Solid Earth, 106, 6325-6345.

Zapata, T.R., Allmendinger, R.W., 1996. Thrust-front zone of the Precordillera, Argentina: a thick-skinned triangle zone. American Association Petroleum Geologists Bulletin, 80, 359-381.

Highlights:

- *Regional and detailed gravimetric analysis was useful to reveal blind oblique structures*
- *Buried oblique structures segment the N-S Precordillera fold and thrust belt system*
- *W-E Divisadero Coba Fault separates two N-S elongated and opposite river basins*
- *La Cantera Fault System continues to the north as a blind structure*

Declaration of interests

- The authors declare that they have no known competing financial interests or personal relationships that could have appeared to influence the work reported in this paper.
- The authors declare the following financial interests/personal relationships which may be considered as potential competing interests:

Journal Pre-proof